



Published in final edited form as:

Mol Cell. 2023 January 05; 83(1): 74–89.e9. doi:10.1016/j.molcel.2022.11.021.

Ring domains are essential for GATOR2-dependent mTORC1 activation

Cong Jiang^{1,7}, Xiaoming Dai^{1,7}, Shaohui He², Hongfei Zhou², Lan Fang³, Jianping Guo¹, Songlei Liu⁴, Tao Zhang¹, Weijuan Pan⁵, Haihong Yu³, Tianmin Fu⁶, Dali Li⁵, Hiroyuki Inuzuka¹, Ping Wang³, Jianru Xiao^{2,*}, Wenyi Wei^{1,8,*}

¹Department of Pathology, Beth Israel Deaconess Medical Center, Harvard Medical School, Boston, MA 02115, USA

²Joint Research Center for Musculoskeletal Tumor of Shanghai Changzheng Hospital and University of Shanghai for Science and Technology, Spinal Tumor Center, Department of Orthopedic Oncology, Shanghai Changzheng Hospital, Shanghai 200003, China.

³Tongji University Cancer Center, Shanghai Tenth People's Hospital, School of Medicine, Tongji University, 200092 Shanghai, China

⁴Department of Genetics, Harvard Medical School, Boston, MA 02115, USA

⁵Shanghai Key Laboratory of Regulatory Biology, Institute of Biomedical Sciences and School of Life Sciences, East China Normal University, 200241 Shanghai, China

⁶Department of Biological Chemistry and Pharmacology, The Ohio State University, Columbus, OH 43210, USA

⁷These authors contributed equally to this work.

⁸Lead Contact

Abstract

The GATOR2-GATOR1 signaling axis is essential for amino acid-dependent mTORC1 activation. However, the molecular function of the GATOR2 complex remains unknown. Here we report that disruption of the Ring domains of Mios, WDR24 or WDR59 completely impedes amino acid-mediated mTORC1 activation. Mechanistically, via interacting with Ring domains of WDR59 and WDR24, the Ring domain of Mios acts as a hub to maintain GATOR2 integrity, disruption

*Correspondence: Jianru Xiao83@163.com (J.X.), wwei2@bidmc.harvard.edu (W.W.).

AUTHOR CONTRIBUTIONS

C.J. and X.D. designed the research plan and performed almost all the experiments with assistance from S.H., H.F.Z., L.F., J.G., J.V., S.L., T.Z., B.W., W.P., H.Y., T.F., S.L. and W.P. help with the imaging analysis. L.F., H.Y., D.L. help with mice generation and phenotype analysis. J.X. and W.W. guided the study. C.J., X. D., and P.W., S.G., J.X. and W.W. wrote and edited the manuscript.

SUPPLEMENTAL INFORMATION

Supplemental information includes 6 supplemental figures.

DECLARATION OF INTERESTS

W.W. is a co-founder and consultant for the ReKindle Therapeutics. Other authors declare no competing financial interests.

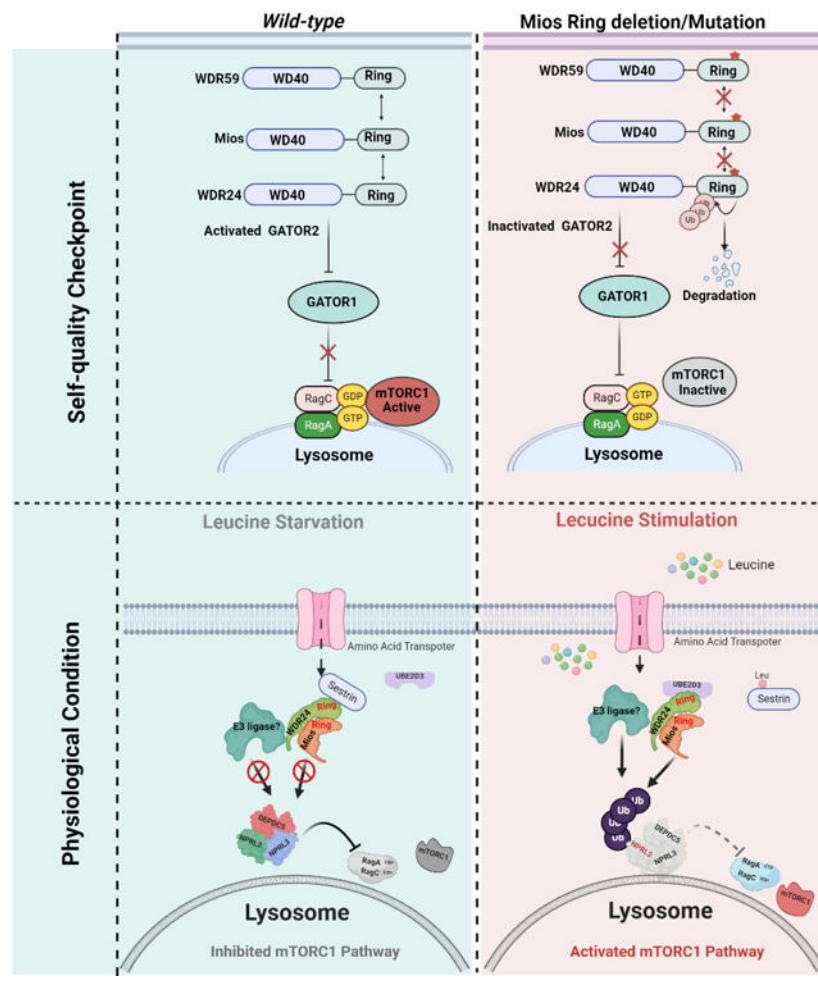
Publisher's Disclaimer: This is a PDF file of an unedited manuscript that has been accepted for publication. As a service to our customers we are providing this early version of the manuscript. The manuscript will undergo copyediting, typesetting, and review of the resulting proof before it is published in its final form. Please note that during the production process errors may be discovered which could affect the content, and all legal disclaimers that apply to the journal pertain.

of which leads to self-ubiquitination of WDR24. Physiologically, leucine stimulation dissociates Sestrin2 from the Ring domain of WDR24 and confers its availability to UBE2D3 and subsequent ubiquitination of NPRL2, contributing to GATOR2-mediated GATOR1 inactivation. As such, *WDR24* ablation or Ring deletion prevents mTORC1 activation, leading to severe growth defects and embryonic lethality at E10.5 in mice. Hence, our findings demonstrate that Ring domains are essential for GATOR2 to transmit amino acid availability to mTORC1 and further reveal the essentiality of nutrient-sensing during embryonic development.

In Brief

Ring domain of Mios acts as a hub to maintain GATOR2 integrity, disruption of which leads to self-ubiquitination of WDR24, while leucine stimulation potentiates the E3 ligase activity of WDR24 via impeding Sestrin2 binding to the Ring domain of WDR24 to confer its availability to the E2 enzyme UBE2D3 and subsequent ubiquitination of NPRL2, a process that is likely essential for leucine-dependent activation of mTORC1.

Graphical Abstract



INTRODUCTION

mTORC1 is a central regulator that integrates diverse environmental cues to potentiate the anabolic process including protein synthesis and attenuate the catabolic process such as autophagy, through which dictates a plethora of cellular processes including cell growth and homeostasis^{1,2}. Aberrant activation of the mTORC1 signaling pathway contributes to many human diseases, including cancer, diabetes and neurological disorder^{1,3,4}. mTORC1 is activated only when both the nutrients and growth factors signal are present¹. Amino acids promote the translocation of mTORC1 to the lysosome surface via the Rag guanosine triphosphatases (Rag GTPases), which is a prerequisite step in the activation of mTORC1^{5,6}. The lysosomal resided GTPase, Rheb, subsequently stimulates the kinase activity of mTORC1 and eventually leads to the activation of mTORC1 signaling⁷. Growth factors dictate the activation of Rheb via dissociating its GAP TSC (TSC1-TSC2- TBC1D7) complex from the lysosomal surface⁸.

Multiple protein complexes have been identified to regulate the amino acid sensing of mTORC1. Regulator anchors Rag GTPase heterodimer to the lysosomal surface and coordinates with SLC38A9 to regulate its nucleotide state⁹⁻¹⁴. GATOR1 complex functions as a GTPase-activating protein (GAP) for RagA/B, while the FLCN-FNIP complex is a GAP for Rag C/D^{15,16}. KICSTOR complex is required for GATOR2 complex to interact and antagonize GATOR1 GAP activity^{15,17-19}. Furthermore, Sestrin2, SARB1, and Castor1 could sense and bind to cytosolic leucine and arginine, respectively, which subsequently causes their dissociation with GATOR2, relieving their inhibitory impact on GATOR2²⁰⁻²².

Despite the establishment of the GATOR2-GATOR1-Rag axis as the major signaling components to regulate the activation of mTORC1 by amino acids, the mechanistic basis for this regulation remains poorly defined. Within the GATOR1 complex, NPRL2 links NPRL3 and DEPDC5 and acts as a GAP for RagA²³. Two interaction modes are likely involved in the regulation of Rag GTPase by GATOR1 complex: 1) DEPDC5 directly interacts with RagA and antagonizes GATOR1-mediated stimulation of the GTP hydrolysis by RagA; 2) the NPRL2-NPRL3 heterodimer interacts with RagA with a weaker affinity and execute its GAP activity^{23,24}. GATOR2 complex comprises five subunits, WDR24, WDR59, Mios, SEC13 and SEH1L, functioning as a key node of the amino acid sensing pathway which links the upstream amino acid sensing to the timely activation of mTORC1 at the lysosome. However, the molecular function of GATOR2 remains enigmatic to date (Figure 1A).

Here, we report that Ring domains of Mios, WDR24 or WDR59 (GATOR2 Ring contained subunits) are essential for amino acid-mediated mTORC1 activation. Ring domain of Mios acts as a hub for the integrity of the GATOR2 holo-complex and functions as a brake to prevent the self-ubiquitination of WDR24; whereas the Ring domain of WDR59 or WDR24, by engaging with Mios Ring domain, mediates the intra-molecular interaction within the complex. Furthermore, we found that leucine stimulation disassociates Sestrin2 with the Ring domain of WDR24 and the induced conformational changes in Ring domain interface of Mios and WDR24, facilitating the E2 (UBE2D3) loading of WDR24 for its activation and subsequently ubiquitination of NPRL2. Wdr24 Ring deletion phenocopied *Wdr24* deficiency

accompanied with decreased mTORC1 activity in *vivo*, revealing the critical role of amino acids sensing in embryonic development.

RESULTS

Ring domains of GATOR2 complex are critical for amino acid-mediated mTORC1 activation

To interrogate the molecular function of GATOR2, we utilized the CRISPR-Cas9 system to insert an in-frame Flag-tag at the endogenous *WDR24* gene locus in HEK 293 cells to ensure physiological immunoprecipitation of the GATOR2 complex (Figures S1A–1B). Consistent with previous studies^{15,17,18}, we found that amino acid availability displays no detectable impact on the integrity of the GATOR2 complex as well as its interaction with the GATOR1 complex evidenced by the co-immunoprecipitation assay (Figure S1C) and the size-exclusion chromatography (SEC) analysis (Figure S1D).

GATOR2 is an evolutionarily conserved protein complex composed of five subunits, WDR24, WDR59, Mios, Sec13 and Seh1L (Figure 1B)¹⁵. Protein sequence alignment revealed that all five known GATOR2 components contain multiple tandem WD40 domains at the N-terminus, which are arranged into β -propeller structure. Notably, WDR24, WDR59 and Mios contain a putative C-terminal Ring domain preceded by the β -propeller and α -solenoid stretch and share similar fold arrangements with the HOPS complex and the CORVET complex (Figure 1B and Figures S1E–1F)^{25,26}. RING domain is a key protein-protein interaction module that has been shown to engage in the interaction mode of various regulatory proteins or associate with E3 ubiquitin ligase activity via recruiting the ubiquitin-conjugating E2 enzyme^{27–30}. WD40-repeat units (beta-propeller) likely also serve as a rigid scaffold for protein interaction and are critical for coordinating the assemblies of a multi-protein complex, which have already been observed in E3 ubiquitin complexes such as the Cullin-Rbx1-SCF complex^{31,32}. We thus investigated whether the beta-propeller or Ring domain of Mios, WDR24 and WDR59 is required for mTORC1 activation. Notably, we found that either ablating the beta-propeller domain or Ring domain of Mios, WDR24, and WDR59 blunted amino acid sensing of mTORC1 signaling as evidenced by the phosphorylation of S6K (Figures S1G–1I). Given that the beta-propeller domain is composed of multiple WD40 units (300 aa), which is much bigger than the Ring domain (50 aa), it is likely very complicated to elucidate its exact functions without detailed structural insights. Moreover, Ring containing proteins Vps11 and Vps8 have been shown to play important roles in mediating the biological functions of the HOPS/CORVET complexes^{33,34}, which prompted us to firstly consider a possible role of Ring domains in mediating GATOR2's molecular function.

To identify the putative functional residues in the Ring domain of Mios, WDR24 and WDR59, we aligned the sequence with the well-defined Ring-H2 E3 ubiquitin ligase Rbx1 (Figure 1B and Figures S1J–1L)³⁵, and mutated the first two conserved critical cysteine residues to alanine, generating *Mios*^{C785A/C788A}, *WDR24*^{C743A/C746A} and *WDR59*^{C924A/C927A} mutants (referred to as CA hereafter), respectively. We then reconstituted *Mios*^{-/-}, *WDR24*^{-/-} and *WDR59*^{-/-} cells with the respective wild-type, RING domain deletion (Ring) or CA mutation transgenes and assessed whether the Ring domains were required for GATOR2 function in amino acid-mediated mTORC1 activation. Notably, *Mios*-deficient

cells stably expressing the Mios Ring deletion or Mios CA mutant failed to restore mTORC1 sensitivity to amino acids as evidenced by the phosphorylation status of S6K (Figure 1C). Furthermore, lysosome recruitment of mTORC1 was abolished in these mutant cells (Figure 1D and Figure S1M), which was a critical step for mTORC1 activation upon amino acid stimulation^{6,36}. In addition, in keeping with previous results^{17,18}, we found that depletion of *Mios* leads to destabilization of WDR24, but not WDR59, and the Ring-defective mutants of Mios were incapable of stabilizing WDR24 levels (Figure 1C), which possibly explains its deficiency in amino acid-induced mTORC1 activation (Figures 1C–D and Figure S1M). Similarly, in comparison with the wild-type reconstituted *WDR24*^{-/-} or *WDR59*^{-/-} cells, Ring deletion or CA mutation form of WDR24 or WDR59 was unable to correct the insensitivity of mTORC1 to amino acids as indicated by the phosphorylation of S6K (Figure 1E and 1G) and the mTORC1 lysosome translocation (Figure 1F and 1H and Figures S1N–1O). However, WDR24 or WDR59 Ring mutants did not affect the protein levels of other subunits (Figures 1E–1G), which differs from that of Mios. The observation that all the Ring domain defective mutants of Mios, WDR24 and WDR59 failed to transmit the positive signal from amino acids to mTORC1 indicated a pivotal role for the Ring domains in GATOR2-mediated amino acid sensing of mTORC1.

Genetic mutation of core residues in WDR24 or WDR59 Ring domain impairs amino acid-mediated mTORC1 activation

Given that Ring domain of Mios behaves differently from that of WDR24 and WDR59, which presumably regulates mTORC1 activation via modulating the protein levels of WDR24, we further dissected the physiological role of the Ring domain via introducing cysteine to alanine mutations into *WDR59* and *WDR24* gene locus at the endogenous level by CRISPR/Cas9 system (Figures S2A–2D). In comparison with parental cells, *WDR24*^{C743A/C746A} or *WDR59*^{C924A/C927A} knock-in cells showed detectable deficiency in amino acid-mediated mTORC1 activation as assessed by the phosphorylation of S6K, S6 and 4EBP1 (Figures 2A–2B). GATOR2 is essential for transmitting the leucine or arginine signal to mTORC1 via disassociating with the cognate sensor, Sestrin2 and Castor1^{20,21}. In keeping with this notion, Ring mutation of WDR24 and WDR59 prevented leucine or arginine-stimulated mTORC1 activation as revealed by the phosphorylation of its downstream substrate S6K (Figures S2E–2F). On the other hand, Rag GTPase-mediated mTORC1 lysosome recruitment is a critical step for amino acid-induced activation^{5,6,36}. Accordingly, disruption of the Ring domain of WDR24 or WDR59 also led to defective mTORC1 localization to lysosome surface in response to amino acid stimulation (Figures 2C–2D and Figures S2G–2H). Consequently, compared with WT-parental cells, *WDR24*^{C743A/C746A} or *WDR59*^{C924A/C927A} showed a noticeable reduction in cell size (Figures S2I–2J) and activated autophagy as evidenced by the increased LC3B (Figures S2K–2L). Moreover, impaired mTORC1 activation in *WDR24*^{C743A/C746A} or *WDR59*^{C924A/C927A} cells was largely prevented either by NPRL2 deficiency or expressing a constitutively active form of Rag GTPases (RagA^{Q66L}/RagC^{S75N}) (Figures 2E–2F)⁶, suggesting that these defects likely stem from the inactivation of Rag GTPase and subsequent impaired recruitment of mTORC1 to lysosome surface. Thus, these results further confirmed the requirement of WDR24 or WDR59 Ring domains for the GATOR2 complex to transmit the amino acid availability signal to mTORC1.

Ring domains of GATOR2 complex are critical for GATOR2 integrity

We next explored the underlying molecular mechanism by which the Ring domains of Mios, WDR24 and WDR59 are critical for the GATOR2-dependent mTORC1 activation. Since Ring domain is an essential module that is best known for implicating in protein-protein interaction²⁷, we went on to explore whether the Ring domain was involved in modulating the interaction of different subunits within GATOR2 complex via an *in vitro* reconstituted system. To this end, we recombinantly expressed and purified GST-fusion protein encoding the full-length wild-type Mios, the Ring domain only (Mios Ring), Mios- Ring, and Mios with the C785A/C788A mutant, and incubated these mutants with other GATOR2 subunits (WDR24, WDR59, Sec13 and Seh11) that were purified from 293T cells. Notably, full-length Mios and Mios Ring were able to pull down WDR24 and WDR59, whereas Mios- Ring and CA mutants failed to bind the corresponding subunits *in vitro* (Figure 3A). Subsequently, the interaction mode of the WDR24 and WDR59 Ring domain were similarly explored. Notably, full-length WDR24 was able to pull down Mios, while mutating the Ring domain blunted its interaction with Mios (Figure 3B). Similarly, the Ring domain of WDR59 was also necessary and sufficient for the binding with Mios (Figure 3C).

Given the potential role of Ring domain in mediating protein-protein interactions, we proceeded to directly assess the interaction between Mios Ring domain with the Ring domain of WDR24 or WDR59. In support of this notion, the GST-Mios Ring domain was able to pull down WDR24 or WDR59 Ring domain as assessed by *in vitro* pull-down assay (Figures 3D–3E). We further implemented the NanoBit-based interaction assay to monitor the Ring-Ring domain interaction in cells³⁷. Our results showed that Mios Ring domain interacted with WDR24 and WDR59 Ring domain in cells (Figure S3C–S3F), while mutating the conserved critical residues (CA mutation) dramatically reduced their binding affinity (Figures 3F–3G and Figures S3G–3H). Overexpression of WDR59 Ring domain exerts no effect on the interaction between WDR24 and Mios Ring domain (Figure S3I), indicating that WDR24 and WDR59 simultaneously engage with Mios Ring domain. Taken together, these results demonstrated the requirements of the Ring domain in mediating the intra-molecular interaction of Mios, WDR24 and WDR59, to maintain the integrity of the GATOR2 complex.

WDR24 has intrinsic E3 ubiquitin ligase activity

Interestingly, in keeping with the previous observations^{17,18}, we found that the WDR24 protein level was dramatically reduced in *Mios* knockdown cells (Figure 1C). Proteasome inhibition via treating cells with MG132, Bortezomib, or TAK-243, but not with the autophagy inhibitor chloroquine (CQ), elevated WDR24 protein levels in *Mios* knockdown cells (Figures S3J–S3K). These results suggest that ubiquitination-mediated post-translational modification is likely involved in modulating the protein abundance of WDR24 in this experimental setting. In support of this notion, enhanced ubiquitination of WDR24 was observed in *Mios*-knockdown cells (Figure S3L). Notably, Ring domain could also recruit a ubiquitin-conjugating E2 enzyme to mediate self-ubiquitination or attach ubiquitin chains to other substrates^{30,38}. In keeping with this notion, WDR24 was able to generate ubiquitin chains *in vitro*, whereas mutating the Ring domains (Ring deletion or CA mutation) abolished this capability (Figures S3M–3N), indicating that WDR24

likely possesses the intrinsic E3 ubiquitin ligase activity *in vitro*. Furthermore, we found that WDR24 self-ubiquitination and WDR24 disappearance required its E3 activity as depletion of *Mios* led to WDR24 destabilization in WT, but not in *WDR24^{C743A/C746A}* cells, in the absence of *Mios* (Figure 3H). To further determine whether the reduction of WDR24 protein abundance in *Mios*-deficient cells is responsible for the observed loss of mTORC1 activation, we reconstituted *Mios*-deficient cells with WDR24 or *Mios* (as a control). Reconstitution with WDR24 failed to restore mTORC1 sensitivity to amino acids (Figure S3O). Furthermore, in the absence of *Mios*, WDR24 was unable to bind to the other subunits of GATOR2 despite being reconstituted comparable to endogenous levels (Figure S3P). This result implies that except for regulating WDR24 protein abundance, *Mios* has other functions in the regulation of mTORC1 activity. In addition, in *Mios*-deficient cells, ectopically expressed *Mios* Ring deletion or CA mutants were unable to bind to other GATOR2 components, correlating with increased ubiquitination and reduction in protein abundance of WDR24 (Figure 3I). In keeping with this finding, *Mios* Ring domain, but not the CA mutant, could strongly block the self-ubiquitination of WDR24 *in vitro* (Figure S3Q). Therefore, the Ring domain of *Mios* is likely required for GATOR2 assembly and functions as a brake to prevent WDR24 from engaging the potential E2 enzyme via its Ring domain to mediate its self-degradation (Figure 3J), acts as a self-quality checkpoint to ensure that the GATOR2 complex is well-integrated to exert its biological function in mTORC1 regulation that is also observed in LUBAC E3 ubiquitin ligase complex^{39,40}.

WDR24 ubiquitinates NPRL2 upon amino acid stimulation

Notably, we found that the ubiquitination levels of NPRL2, the catalytic subunit of GATOR1, but not NPRL3 or DEPDC5, were physiologically regulated in an amino acid-sensitive manner in our experimental setting (Figures S4A–S4F). Amino acid stimulation induced the ubiquitination of NPRL2 in the intact GATOR1 complex without affecting the protein stability or the integrity of GATOR1 complex (Figure S4G). Depletion of *WDR24* blunted the increased ubiquitination levels of NPRL2 upon amino acid stimulation (Figure 4A). On the other hand, ectopic overexpression of WDR24 promoted ubiquitination of NPRL2 in a Ring domain-dependent manner (Figure S4H). In keeping with this finding, defective NPRL2 ubiquitination in *WDR24^{-/-}* cells was largely restored by re-expressing wild-type WDR24, but not by the Ring mutation (CA mutant) form of WDR24 (Figure 4B). In further support of the critical role of WDR24 in mediating NPRL2 ubiquitination, deletion of *Mios* or *Mios* Ring domain blunted amino acid-induced NPRL2 ubiquitination (Figures S4I–4J). This is probably caused by the fact that complete deletion of *Mios* or the *Mios*-Ring domain leads to the destabilization of WDR24, thereby conferring NPRL2's unavailability to WDR24 and other GATOR2 subunits, which eventually leads to the deficient NPRL2 ubiquitination in these cells (Figure S4K). Mutation of the Ring domain of WDR59 inhibits GATOR2-mediated ubiquitination of NPRL2 in cells (Figure S4L), indicating the integrity of GATOR2 is critical for amino-acids induced NPRL2 ubiquitination.

We next sought to determine the type of ubiquitin chain that was generated on NPRL2 in *NPRL2^{HA}* knock-in HEK293 cells. We found that WDR24 generated K6, K11, K48 and K63 chains *in vitro* via using self-ubiquitination as a readout (Figure S4M). Furthermore,

NPRL2 could be labeled only with wild-type or K6 ubiquitin (ubiquitin mutant contains only one lysine) via over-expressing GATOR2 in cells (Figure S4N). Moreover, K6R (Lys⁶→Arg⁶) ubiquitin inhibited amino acid stimulation-induced NPRL2 ubiquitination (Figure 4C), indicating that GATOR2 likely promotes K6-linked ubiquitination of NPRL2. To further demonstrate the requirement of K6-linked ubiquitination for amino acid sensing, we used a previously developed inducible ubiquitin replacement system in which the endogenous ubiquitin was replaced with different K-R mutation variants controlled by doxycycline. Reintroduced K6R, but not the wide-type ubiquitin, impaired mTORC1 activation (Figure 4D). We next sought to identify the critical lysine residue for the NPRL2 ubiquitination. There are 25 lysine residues in NPRL2 (Figures S4O–S4P). Several lysine residues have been previously identified to be ubiquitinated^{41–43}, and conservation alignment indicated that the K158 is highly conserved from mammals to yeast, while the K328 and K357 are well conserved except for yeast (Figure S4Q). We utilized a mutagenesis approach to inactivate individual lysine residues on NPRL2 identified by mass spectrometry. Notably, mutation of K158 or K357 (but not other lysine residues) to arginine, either alone or in combination, decreased GATOR2-mediated ubiquitination of NPRL2 (Figure S4R), whereas the protein turnover rates of the K158/357 mutants were similar to that of wild-type NPRL2 (Figure S4S). More importantly, mutating these two conserved lysine residues, K158 and K357 at NPRL2, impaired amino acid-mediated ubiquitination of NPRL2 (Figure 4E) and mTORC1 activation as indicated by the phosphorylation of S6K, 4EBP1 and TFEB (Figure 4F) and the lysosome recruitment of mTORC1 (Figure 4G).

In keeping with the reduced mTORC1 kinase activity, cells expressing the ubiquitination-deficient *NPRL2* mutant displayed activated autophagy and reduced cell size (Figures 4H–4I). Furthermore, genetic ablation of *WDR24* prevented the reduced GATOR1-binding RagA under amino acid stimulated condition (Figure 4J). In support of this finding, amino acid addition failed to disrupt NPRL2 interaction with RagA in cells expressing the ubiquitination deficient NPRL2 (K158/357R) mutant and consequently inhibited the GAP activity of GATOR1 as evidenced by the reduction in GTP-form of RagA (Figure 4K). Thus, our data provide multiple lines of evidence corroborating the formation of a K6-linked polyubiquitin chain on NPRL2 at the K158 and K357 residues, which is mediated by the WDR24 subunit of GATOR2 complex.

Ring domain of WDR24 is essential for its interaction with Sestrin2

Under physiological conditions, GATOR2 is inhibited by its interaction with Sestrin2, Castor1^{20,21}. Hence, we continued to ask whether these proteins could interact with the ring domains of GATOR2 subunits. Notably, we found that Sestrin2 directly bound to the GATOR2 complex via WDR24 and WDR59 subunits (Figure 5A), whereas Castor1 interacted with all the four subunits, except for Sec13, which appears to be in a more complicated manner (Figure S5A). We thus focused on the leucine sensor Sestrin2 for the remainder of the study. We observed that genetic ablation of *WDR24* prevented the interaction between WDR59 and Sestrin2, while loss of *WDR59* did not obviously change the binding of WDR24 with Sestrin2 (Figure 5B and Figure S5B). Thus, WDR24 is likely the key subunit to bridge the association of the GATOR2 complex and Sestrin2. Further analysis showed that the WDR24 Ring domain is essential but not sufficient to interact

with Sestrin2 (Figure 5C and Figures S5C–S5D). WDR59 Ring domain behaved the same as the WDR24 Ring domain in mediating the integrity of GATOR2 complex¹⁹. However, unlike the Ring deletion mutant of WDR24, WDR59 Ring deletion mutant still interacts with Sestrin2 (Figure S5E), excluding the possibility that WDR24 Ring deletion induced disassemble of GATOR2 complex, which subsequently prevented Sestrin2 from binding to GATOR2 complex. More importantly, deletion of *Sestrin1*, *Sestrin2*, and *Sestrin3* in cells led to constitutive ubiquitination of NPRL2 in cells (Figure 5D), indicating that Sestrin2 could potentially antagonize GATOR2-mediated NPRL2 ubiquitination in this experimental setting.

To identify the E2 enzyme(s) that is critically involved in WDR24 E3 ligase activity, we performed an siRNA screen to determine the E2 enzyme required for amino acid-mediated mTORC1 activation (Figure S5F). Genetic ablation of seven E2 enzymes (*UBE2D3*, *UBE2G1*, *UBE2J2*, *UBC13*, *UBE2Q2*, *UBE2QL1*, and *UBE2W*) impaired amino acid-mediated mTORC1 activation (Figure S5G). We next used NPRL2 ubiquitination as another readout and found that depletion of *UBE2J2* and *UBE2D3* impaired NPRL2 ubiquitination and mTORC1 activation in cells, which suggests that *UBE2J2* and *UBE2D3* coordinately regulate the ubiquitination of NPRL2 (Figure S5H). Moreover, *in vitro* reconstituted GATOR1 and immunopurified GATOR2 prepared from amino acid stimulation conditions poly-ubiquitinates NPRL2 in cooperation with *UBE2D3* and with *UBE2J2 in vitro* (Figure 5E and Figures S5I–S5K). Importantly, we found that the E3 ligase activity of purified GATOR2 was found to be relatively weak compared to the positive control *UBE4B* (Figure S5J), which may likely be caused by the fact that WDR24 lacks the linchpin arginine that is essential for coordinating with *UBE2D* family E2s to prime the donor ubiquitin transfer^{44–46}, or other mechanisms such as post-translational modification may be involved in governing GATOR2 E3 ligase activity in cells. Furthermore, we found that WDR24 specifically bound to *UBE2D3 in vitro* (Figure 5F), and wild-type Sestrin2 interrupted the interaction of WDR24 with *UBE2D3* and inhibited the self-ubiquitination of WDR24 *in vitro* (Figures S5L–5M). The addition of leucine, which can block the interaction of WDR24 with Sestrin2, restored its interaction with *UBE2D3 in vitro*, whereas L261A-Sestrin2 (leucine insensitive) mutant constantly blunted the interaction between *UBE2D3* and WDR24 *in vitro* (Figure 5G). In keeping with this notion, reintroducing the wildtype, but not the GATOR2 binding deficient mutant S190W-Sestrin2, rescued this defect, while the L261A-Sestrin2 mutant strongly inhibited the ubiquitination of NPRL2 in a leucine-insensitive manner (Figure 5H). Moreover, the non-ubiquitinable NPRL2 (K158/357R) impaired leucine-mediated mTORC1 activation as indicated by the phosphorylation of S6K (Figure S5N).

Ring domains interact with the ubiquitin-charged E2 via the conserved surface at the L1 and L2 zinc-coordinating loops and the central α -helix^{31,38}. We next designed a Ring mutant via substitution of conserved hydrophobic E2 binding residue, W772 (α -helix) or V745 (L1 loop) to Alanine or Aspartate to disrupt its interaction with E2^{19,30}, but maintain the folding of the Ring domain (Figures S5O–5P) mutation of V745 or W772 to Alanine (A) or Aspartate (D) alone or in combination reduced its interaction with *UBE2D3 in vitro* (Figure S5Q). WDR24 dimerized with Mios via the Ring-Ring interface and Ring-solenoid interactions to maintain the integrity of GATOR2 complex (Figures S5R–5S)¹⁹. To exclude

the interference of the endogenous GATOR2¹⁹, we analyzed whether these mutants could potentially perturb its association with Mios in *WDR59* knock-out cells. Unlike the WDR24 Ring deletion mutant, these single or double mutants of WDR24 did not obviously affect their binding affinity with Mios (Figure S5T). Moreover, our results showed that mutation of V745 or W772 to Alanine (A) or Aspartate (D) alone reduced amino acid-mediated mTORC1 activation. Notably, we found that these double mutants exhibited a stronger mTORC1 activation defect than either the V745 or W772 single mutant, which behaved comparably to the WDR24 Ring deletion mutant (Figure 5I and Figure S5U). In keeping with these findings, our results showed that disruption of the E2 binding decreased amino acids-induced NPRL2 ubiquitination, but to a lesser extent than the Ring deletion mutant, indicating that except for WDR24, other E3 ligases might also contribute to NPRL2 ubiquitination via engaging with the GATOR2 complex (Figure 5I). However, knocking down of *NEDD4*, a E3 ubiquitin ligase that interacts with UBE2D3^{47,48}, did not affect amino acid induced NPRL2 ubiquitination and mTORC1 activation (Figure S5V), excluding the possibility that NEDD4 is required for the NPRL2 ubiquitination. Taken together, these results implicate that leucine prevents Sestrin2 from binding to the Ring domain of WDR24, leaving the Ring domain to recruit UBE2D3 and subsequently ubiquitinates NPRL2 (Figure 5J).

WDR24 Ring domain deletion mice are embryonic lethal with reduced mTORC1 kinase activity

Since the Ring domain of Mios, WDR59 and WDR24 functions equivalent in the cellular levels, and Mios ring mutations likely inactivate mTORC1 via WDR24 destabilization, we next used a genetic approach to untangle the physiological role of Ring domain of GATOR2 *in vivo* by generating *Wdr24* deficient mice (*Wdr24*^{-/-}) targeting exon 1 and the Ring deletion in mice (*Wdr24*^{Ring/ Ring}) via deleting the Ring domain at exon 7 (Figures S6A–S6B). While *Wdr24*^{+/-} and *Wdr24*^{+/ Ring} mice were viable, deficiency or Ring deletion of *Wdr24* both led to embryonic lethality around E10.5 (Figures S6C–S6D) and resulted in severely decreased body size (Figures 6A–6B and Figures S6E–S6H), was evocative of the phenotypes of that were observed in *RagA*-deficient mice⁴⁹. Consistent with the key role of *Wdr24* Ring domain in cells, mTORC1 activity was severely reduced in the total protein extracts derived from *Wdr24*^{-/-} or *Wdr24*^{Ring/ Ring} mice, as represented by the phosphorylation levels of S6K, S6 as well as 4EBP1 without affecting the protein abundance of NPRL2, NPRL3 and DEPDC5 (Figures 6C–6D and Figures S6I–6J). NPRL2 ubiquitination levels were decreased in *Wdr24*^{-/-} or *Wdr24*^{Ring/ Ring} tissues (Figure S6K), further demonstrating that WDR24 regulates the ubiquitination of NPRL2 at the physiological levels. Compared with the wild-type littermates, *Wdr24*^{-/-} or *Wdr24*^{Ring/ Ring} mice showed severe defects in the development of fetal liver and heart (Figure S6L). Furthermore, immunohistochemical detection of phospho-S6 in liver and heart sections revealed decreases in mTORC1 activity and increases in apoptosis as assessed by cleaved caspase-3 staining (Figures 6E–6F and Figures S6M–6P).

We then established mouse embryonic fibroblasts (MEF) cells from *Wdr24*^{-/-} or *Wdr24*^{Ring/ Ring} mice to further explore the role of *Wdr24* Ring domain in amino acid sensing. In comparison with the parental cells, amino acid-mediated mTORC1 activation

was impaired in *Wdr24*^{-/-} or *Wdr24*^{Ring/ Ring} MEF cells (Figure S6Q). In keeping with the phenotypes observed from *WDR24*^{C743A/C746A} or *WDR59*^{C924A/C927A} expressing HEK293 cells (Figures S2E–S2F), leucine or arginine stimulated mTORC1 activation was strongly blunted in *Wdr24* Ring deletion MEF cells (Figure S6R). In cells lacking *Wdr24* or expressing the Ring deletion mutant, mTOR diffused in the cytoplasm regardless of the presence or absence of amino acids (Figures S6S–6T). To position the WDR24 Ring function in mTORC1 pathway, we performed epistasis analysis. Notably, deletion of the endogenous *Nprl2* or expressing the constitutively active mutant heterodimer of Rag GTPase (RagA^{Q66L}/RagC^{S75N}) corrects the mTORC1 inactivation in WDR24 Ring cells (Figure 6G). Taken together, *Wdr24* Ring deletion phenocopied *Wdr24* deficiency *in vivo*, with decreased mTORC1 activity in multiple tissues, revealing the critical role of amino acids sensing in embryonic development (Figure 6H).

DISCUSSION

GATOR2 is a positive regulator of the nutrient-sensing of mTORC1 signaling, transmitting the amino acid signal from the leucine sensor Sestrin2 or arginine sensor Castor1 to the GATOR1-Rag GTPase axis. One unsolved question in the amino acid sensing field revolves around how Sestrin2 and Castor1 inhibit GATOR2, which awaits elucidation of the molecular function of GATOR2. Here we report that the Ring domains of Mios, WDR24 and WDR59 are essential parts of GATOR2-mediated amino acid sensing. Ring domain of Mios is necessary and sufficient for the interaction with WDR24 and WDR59 Ring domains to maintain the integrity of the GATOR2 complex and likely functions as a brake for preventing the self-ubiquitination of WDR24. On the other hand, Ring domains of WDR24 and WDR59 are largely involved in mediating the intra-molecular interaction with Mios Ring domain. More importantly, genetic deletion of WDR24 Ring domain impairs the nutrient-sensing of mTORC1, leading to embryonic lethality and severe growth defects *in vivo*. These observations are largely in line with the independent study from Max L. Valenstein and colleagues' report, which reported the structure of the GATOR2 complex¹⁹.

In addition, we found that WDR24 has intrinsic E3 ubiquitin activity, whose enzymatic activity is largely antagonized via engaging with Mios Ring domain. Disruption of the Ring-Ring interaction of WDR24 and Mios, either by genetic deletion of *Mios* or mutation of Mios Ring domain, will release this inhibitory effect and be fully exposed to the E2 enzyme, which will subsequently lead to the self-degradation of WDR24 (Figure S6U–I). Moreover, we found that WDR24 can promote the ubiquitination of NPRL2 in the overexpression system and *in vitro*. The Ring domain of WDR24 is also required for its interaction with the cytosolic leucine sensor Sestrin2; leucine stimulation dissociates Sestrin2 from the Ring domain of WDR24 and confers its availability to UBE2D3 *in vitro*. Consistently, manipulating the interaction of WDR24 and Sestrin2 affects the ubiquitination levels of NPRL2 in cells. Thus, Mios and Sestrin2 can separately or synergistically bind to distinct sites of WDR24 Ring as the brake to inhibit E2 loading of WDR24 for its activation (Figure S6U–II). Upon leucine stimulation, Sestrin2 disassociates with the Ring domain of WDR24 and the induced conformational changes in Ring domain interface of Mios and WDR24, facilitating the E2 loading of WDR24 for its activation and subsequently ubiquitination of NPRL2 (Figure S6U–III). However, our results demonstrated that NPRL2 ubiquitination

deficient mutants (K158/357R) did not completely impair mTORC1 activation (Figure 4F) as observed in *WDR24* knockout or Ring mutation cells (Figure 1E and Figure 2A) and the immunoprecipitated GATOR2 complex have a much lower activity to generate ubiquitin chains *in vitro* (Figure S5J). Thus, whether WDR24-mediated NPRL2 ubiquitination is a prominent mechanism for GATOR2-mediated GATOR1 inhibition is still elusive. Moreover, our results demonstrated that the beta-propeller domain of Mios, WDR24, and WDR59 are also required for amino acid-induced mTORC1 activation (Figures S1G–1I), indicating that other mechanisms, such as conformational changes, may also play a role in the regulation of GATOR1 by GATOR2. As Castor1 binds to many subunits of GATOR2 (Figure S5A), a more complicated regulatory mechanism is likely involved in the arginine sensing process of the GATOR2 complex.

mTORC1 pathway is hyperactivation in many diseases, and inhibitors of mTORC1 signaling have valuable therapeutic values to target the aberrant mTORC1 signaling^{1,4}. Given that Ring domains are critical for GATOR2-mediated mTORC1 activation, it may be possible to develop small molecules or peptides that antagonize the Ring-Ring interaction of Mios-WDR24 or Mios-WDR59 that specifically target the cytosolic amino acids sensing arm of the mTORC1 pathway.

Limitations of the Study

Our data provide experimental evidence to support the notion that WDR24-mediated ubiquitination of NPRL2 is likely involved in GATOR2-mediated GATOR1 inhibition. However, the significance of the observed mechanism in physiological contexts remains to be further determined. Notably, our results showed that, unlike the WDR24 Ring deletion mutant, the mutation in the E2 binding sites of WDR24 did not fully inhibit amino-acids mediated NPRL2 ubiquitination. This implies that other E3 ligases might also contribute to the ubiquitination of NPRL2 via engaging with the GATOR2 complex, which warrants further investigation. Moreover, the study of Max L. Valenstein *et al* showed that expression of the NPRL2 mutant lacking all the lysine residues restored amino acid-sensitive mTORC1 signalling¹⁹. Given that lysine residue is the receptor of multiple post-translational modifications besides ubiquitination, such as sumoylation, acetylation, methylation, *et al*^{60–52}. It is worthy to further investigate whether other types of modifications might occur on the other lysine residues of NPRL2, which potentially activates GATOR1 and subsequently neutralizes the effect of ubiquitination-mediated regulation of GATOR1 activity. Furthermore, whether other substrates besides NPRL2 contribute to GATOR2-mediated mTORC1 activation remains elusive. In addition, we observed that WDR59 exerts E3 ubiquitin ligase activity *in vitro* (Figure S3L). Hence, whether WDR59 contributes to the ubiquitination of NPRL2 and how the E3 ligase activities of WDR24 and WDR59 are coordinated and whether an additional regulatory factor is involved remains to be further investigated.

It is worth noting that the study of Max L. Valenstein *et al.* suggests that α -solenoid of Mios occludes the putative E2-interacting surface of WDR24, thereby precluding any E2 from associating with WDR24 and subsequently ubiquitinates any substrates¹⁹. However, our results showed that mutation of the E2 binding sites of WDR24 without

affecting the integrity of GATOR2 impaired amino acid-mediated activation (Figure 5I and Figure S5U), indicating that WDR24 might exert E3 ligase activity, independent of its reported role in maintaining GATOR2 integrity, to govern GATOR2-mediated mTORC1 activation under certain conditions. To this end, GATOR2 acts as a hub via intermediating the upstream sensors, Sestrin2 and Castor1, with KICSTOR and GATOR1 at the lysosomal surface^{17,18,20,21}. Hence, GATOR2 may exist in multiple intermediate conformations structures via engaging with sensors or GATOR1-KICSTOR complex (switch from the “OFF” to “ON” state), and there might be rearrangement or conformational change in the Ring- α -solenoid interface, which will enable WDR24 to interact with E2 while disassociating with sensors and engaging with GATOR1/KICSTOR. Atomic structure analysis of the dynamic change of GATOR2 complex from the nutrient-deficient (inactive form, associated with sensors such as Sestrin2) to nutrient-sufficient status (active form, disassociated with sensors such as Sestrin2) as well as the co-structure of the GATOR2-KICSTOR-GATOR1 complex are warranted to gain deeper insights into the possible conformational dynamics of GATOR2, which will further reveal the critical role of the WDR24-RING motif in the dynamic regulation of the GATOR2 to dictate timely mTORC1 activation following physiological upstream cues such as amino acid stimulation.

STAR ★ METHODS

RESOURCE AVAILABILITY

Lead Contact—Further information and requests for resources and reagents should be directed to and will be fulfilled by the Lead Contact, Wenyi Wei (wwei2@bidmc.harvard.edu).

Materials availability—All unique reagents generated in this study are available from the lead contact with a completed Materials Transfer Agreement.

Data and code availability

- All data is available in the main text or the supplemental information.
- This paper does not report original code.
- Any additional information required to reanalyze the data reported in this paper is available from the lead contact upon request.

EXPERIMENTAL MODEL AND SUBJECT DETAILS

Cell lines—HEK293, HEK293T, primary MEF and HeLa cells were cultured in DMEM supplemented with 10% FBS, 100 U ml⁻¹ penicillin/streptomycin. HEK293, HEK293T and HeLa cells were maintained at 37 °C and 5% CO₂. *NPRL2^{Flag}* HEK293T cells and *Sestrin^{1/2/3}* triple knockout were a gift from the lab of Dr. David M. Sabatini. *WDR24^{-/-}*, *WDR59^{-/-}*, and *Mios^{-/-}* HEK293T cells were a gift from Dr. Ming Li (Memorial Sloan Kettering Cancer Center, New York, NY). All the cell lines were authenticated and validated for mycoplasma negative.

Animals—To generate the *Wdr24*^{-/-} mice, guide RNA targeting the *Wdr24* locus on exon1 was designed using the online website (<http://crispr.Mit.edu/>). gRNA (listed in the Oligonucleotides) and *in vitro* translated Cas9 mRNA were co-microinjected into C57BL/6 mice-derived zygotes. We initially wanted to generate the *Wdr24*^{C743A/C746A} knock-in mice. The guide RNA targeting the *Wdr24* locus on exon7 and oligo was designed in the same way as *Wdr24*^{-/-} mice. gRNA and oligos were listed in the Oligonucleotides. Unfortunately, we failed to get the desired knock-in mice after 10 times of injections, and we coincidentally obtained the Ring deletion mice (*Wdr24*^{Ring/ Ring}) mice. Founders were screened by PCR and validated by DNA sequencing. The PCR primers used for *Wdr24*^{-/-} and *Wdr24*^{Ring/ Ring} mice were listed in the Oligonucleotides part. Details of the mice deletion information are included in Figure S6A–6D. All the mice were maintained under appropriate conditions and subject to ethical review at East China Normal University.

METHOD DETAILS

Amino acids starvation and re-stimulation—HEK293, HeLa and primary cells were cultured in DMEM supplemented with 10% FBS. One day before the experiments, cells were plated in 6-cm cultured dishes. On the next day, cells were rinsed twice with ice-cold PBS. Then, cells were incubated in complete amino acids, leucine or arginine-free RPMI1640 supplemented with 10% dialyzed FBS for 60 min, and then restimulated with the corresponding amino acids at the indicated time. The final concentration of amino acids, leucine or arginine, was the same as in RPMI 1640 medium.

Generation of the knockout and knock-in cell lines—To generate the knockout cell lines, guide RNA targeting the indicated gene was cloned into lentiCrispr-V2-Puro (Addgene 52961). HEK293 or HeLa cells were transfected with the indicated sgRNA and selected with puromycin for 3 days. The survival cells were plated in a 96-wells plate with approximately one cell per well. After two weeks, the single clone was expanded and verified via immunoblotting using the respective antibody. The sgRNA targeting sequence for WDR24, WDR59, Mios, Seh1L, Sec13, and NPRL2 were described before (Peng et al., 2017; Wolfson et al., 2017). To generate the knock-in cell lines, the guide RNA targeting specific exons were cloned into LentiCrispr-V2-GFP (Addgene 82416). 500 ng of single-strand DNA and 1000 ng of indicated sgRNA were co-transfected into the HEK293 cells. Twenty-four hours post-transfection, GFP-positive cells were sorted via flow cytometry and plated into 96-well plates. Two weeks later, the clones were expanded and verified using genomic sequencing. The primers and single-strand DNA used to generate the knock-in cells are listed in Oligonucleotides.

Generation of the primary MEF cells—Primary MEF cells were isolated from E10.5 embryos by excluding the head and liver and prepared by digestion with trypsin for 30 min. Cells were maintained in DMEM medium supplemented with 10% fetal bovine serum and followed by serial passage when the cells became confluence. MEFs were infected with pLVX-Flag lentivirus encoding Metap2 (control protein), Flag-RagAQ66L, Flag-RagCS75N, LentiCrispr-V2-sgVector, LentiCrispr-V2-sgNprl2 and selected for stable expression.

Immunoblots and immunoprecipitation—For immunoblots, cells were lysed directly in lysis buffer (50 mM Tris pH 7.5, 120 mM NaCl, 10% glycerol, 0.5% NP-40, 0.1% SDS) supplemented with protease inhibitors (Complete Mini, Roche) and phosphatase inhibitors (phosphatase inhibitor cocktail set I and II, Calbiochem). For immunoprecipitation, cells were lysed in EBC buffer (50 mM Tris pH 7.5, 120 mM NaCl, 0.5% NP-40) supplemented with protease inhibitor (Complete Mini, Roche). The soluble fractions were clarified via centrifugation; 20 μ l of the anti-Flag or anti-HA beads were added to cell lysis and incubated for 2–4 hours at 4 °C. The beads were washed 3 times with the NETN buffer (20 mM Tris, pH 8.0, 100 mM NaCl, 1 mM EDTA and 0.5% NP-40). The immunoprecipitated proteins were denatured by adding 50 μ l 2 X SDS loading buffer and boiling at 100°C for 10 min, resolved by 8–15% SDS-PAGE and analyzed by immunoblotting.

Cell transfection, RNAi, virus infection and stable cell line generation—For transient transfection, the encoding plasmids were transfected into HEK293 and HeLa cells with Lipofectamine (Invitrogen) or PEI (Polysciences) separately. All siRNAs targeting 32 E2 enzymes were purchased from Shanghai Genechem. siRNA (20nM) was transfected into 293T cells using Lipofectamine RNAiMAX (ThermoFisher Scientific, 13778). To generate the lentivirus, HEK293T cells were transfected with the sgRNA or pLenti-encoding plasmids along with psPAX2 and PMD2G packing plasmids using PEI. Twenty-four hours post-transfection, the fresh medium was replaced. Thirty-six hours later, the supernatants were collected and infected the corresponding cell lines. Cells were selected with puromycin (1 μ g/ml), and survival cells were expanded and validated via immunoblotting.

Immunofluorescence assays and cell size analysis—HeLa or HEK293T cells were plated on gelatin-coated coverslips in a 24-well plate. Twenty-four hours later, the coverslips were rinsed twice with ice-cold PBS and fixed with 4% paraformaldehyde at room temperature. Then, the coverslips were washed with PBS three times and incubated with 0.05% Triton X-100 for 15 min. After washing with PBS three times, cells were blocked in 1% BSA for 1 hour at room temperature. The coverslips were incubated with the indicated primary antibodies overnight at 4 °C. After being rinsed three times with PBS, coverslips were subsequently incubated with the secondary antibodies for 1 hour. Images were acquired on a Zeiss LSM 510 Meta confocal system. For quantitative analyses, images were opened with Fiji software, and approximately 50 cells were quantified via Pearson's correlation. To determine the cell size, HEK293 or HeLa cells were seeded on 10 cm dishes at a 40% confluence. After twenty-four hours, cells were harvested and subjected to FACS analysis. The X-axis indicated the relative cell size.

Size-exclusion chromatography (SEC)—Cells were rinsed twice with ice-cold PBS and lysed in lysis buffer (1% Triton X-100, 50 mM HEPES (pH 7.4), 150 mM NaCl, 2.5 mM MgCl₂, 10% glycerol supplemented with protease inhibitor cocktail), soluble fractions were obtained via centrifugation at 12,000g for 20 min. 3 mg supernatant were loaded on Superose 6 Increase 10/300 GL Column (GE Healthcare, 29–0915-96) connected to an AKTA purifier (GE Healthcare). The flow rate was 0.5 ml/min, and 0.3 ml fractions were collected and denatured in 3 X SDS loading buffer and subjected to immunoblot analysis.

Protein expression and purification—His-MBP and GST-tagged GATOR2 subunits and the indicated mutation were induced in *E. coli* BL21 (DE3) strain and were purified using Ni-NTA agarose resin (Qiagen) or Glutathione Sepharose 4B (GE Healthcare Life Sciences). Briefly, cells were grown in LB medium containing 30 µg/mL kanamycin (His-MBP-tag protein), 100 µg/ml ampicillin (GST-tag protein), and 0.5 mM IPTG was added to induce the expression of indicated protein at 16°C for 14 hours when the OD₆₀₀ reached 0.8. Cells were collected by centrifugation and resuspended in lysis buffer (20 mM Tris-HCl (pH 7.4), 300 mM NaCl supplemented with protease inhibitor cocktail) and disrupted by a homogenizer. His-MBP protein was eluted with elution buffer (20 mM Tris-HCl, 250 mM imidazole, 0.15 M NaCl, pH 8.0), and GST-tagged protein was eluted with GSH elution buffer (50 mM Tris-HCl, 10 mM reduced glutathione, pH 8.0). His-MBP-WDR24 Ring, His-MBP-WDR59 Ring, and GST-Mios Ring proteins were further purified by Hitrap Q HP ion-exchange chromatography and gel filtration chromatography (GE Healthcare Life Sciences) and concentrated in a buffer containing 20 mM HEPES, pH 7.5, 150 mM NaCl and 5% glycerol. For the purification of GATOR2 subunits, pRK5-Flag-WDR24, pRK5-Flag-WDR59, pRK5-Flag-Mios, pRK5-Flag-Sec13 and pRK5-Flag-Seh1L were transfected into HEK293T cells. Twenty-four hours post-transfection, cells were lysed in EBC buffer, and the supernatant was spun in a table-top centrifuge (12000 rpm/4°C/30 min). The supernatant was subsequently incubated with anti-Flag beads for 4 hours. The beads were washed 6 times in NETN buffer (20 mM Tris, pH 8.0, 100 mM NaCl, 1 mM EDTA and 0.5% NP-40) and then washed with PBS 3 times. Each subunit was eluted with PBS containing 0.5 mg/mL FLAG peptide, and the elute was further concentrated to 100 µl with a centrifugal filter with a 30 KDa cut-off (Millipore, UFC9100).

In cell ubiquitination assay—For the in cells ubiquitination assays, cells were lysed in denatured buffer (50 mM Tris pH 7.5, 120 mM NaCl, 10% glycerol, 0.5% NP-40, 1% SDS). After sonication, the supernatant was collected and incubated at 100°C for 5 min. Cell lysates were subsequently diluted 10 times with lysis buffer (50 mM Tris pH 7.5, 120 mM NaCl, 10% glycerol, 0.5% NP-40) supplement with protease inhibitors and 10 nm N-ethylmaleimide (NEM, sigma). The diluted lysis was subjected to immunoprecipitation with HA or Flag beads at 4°C for 4 hours. The beads were washed three times with NETN buffer, denatured via adding 2 XSDS loading buffer and subjected to western blotting analysis.

In vitro ubiquitination assay—For the *in vitro* autoubiquitination assay, purified WDR24 and the indicated mutations proteins were incubated with ubiquitin, E1, ATP and UBE2D3 in ubiquitin reaction buffer according to the manufacturer's instruction (Boston BioChem). To assay ubiquitination of NPRL2 *in vitro*, purified NPRL2 in the intact GATOR1 complex, E1, ubiquitin, and E2 were incubated with purified GATOR2 complex at 37°C for 2 hours in the ubiquitin reaction buffer using the Thermomixer R (Eppendorf), terminated by adding 1% SDS and boiled at 100°C for 5 mins. The reaction was diluted 10 times using EBC buffer and subjected to anti-Flag immunoprecipitation for two hours. The ubiquitination of NPRL2 was analyzed via probing with NPRL2 or ubiquitin antibody. The samples were subjected to immunoblot analysis using a ubiquitin antibody.

For the *in vitro* autoubiquitination assay, purified WDR24 and the indicated mutations proteins were incubated with ubiquitin, E1, ATP and UBE2D3 in ubiquitin reaction buffer according to the manufacturer's instruction (Boston BioChem). To assay ubiquitination of NPRL2 *in vitro*, purified NPRL2 in the intact GATOR1 complex, E1, ubiquitin, and E2 were incubated with purified GATOR2 complex at 37°C for 2 hours in the ubiquitin reaction buffer using the Thermomixer R (Eppendorf), terminated by adding 1% SDS and boiled at 100°C for 5 mins. The reaction was diluted 10 times using EBC buffer and subjected to anti-Flag immunoprecipitation for two hours. The ubiquitination of NPRL2 was analyzed via probing with NPRL2 or ubiquitin antibody. The samples were subjected to immunoblot analysis using a ubiquitin antibody.

GATOR1 and GATOR2 complex purification—For the purification of the GATOR1 complex, pRK5-HA-NPRL3, pRK5-HA-DEPDC5 and pRK5-Flag-NPRL2 were co-transfected into HEK293T cells. Twenty-four hours post-transfection, cells were lysed in EBC buffer, and the supernatant was spun in a table-top centrifuge (12000 rpm/4°C/30 mins). The supernatant was subsequently incubated with anti-Flag beads for 4 hours. The beads were washed 6 times in NETN buffer (20 mM Tris, pH 8.0, 100 mM NaCl, 1 mM EDTA and 0.5% NP-40) and then washed with PBS 3 times. GATOR1 complex was eluted with PBS containing 0.5 mg/ml FLAG peptide, and the elute was further concentrated to 100 µl with a centrifugal filter with a 100 KDa cut-off (Millipore, UFC9100). To obtain the GATOR2 complex, pRK5-Flag-WDR24, pRK5-Flag-WDR59, pRK5-Flag-Mios, pRK5-Flag-Seh1L and pRK5-Flag-Sec13 were co-transfection into HEK293T cells and were purified in the same way as for GATOR1 complex. Endogenous GATOR2 complex was precipitated from amino acid stimulated *WDR24^{Flag}* HEK293 cells with Flag-beads.

Pull-down assay—1 µg GST-Mios Ring protein was incubated with 30 µl Glutathione Sepharose 4B resin in the EBC buffer (50 mM Tris pH 7.5, 120 mM NaCl, 0.5% NP-40) supplemented with protease inhibitor (Complete Mini, Roche) for 3 hours at 4°C. Beads were washed and incubated with 1 µg His-MBP-WDR24 Ring or His-MBP-WDR59 Ring for 1 hour at 4°C. After extensively washing with low salt NETN buffer (20 mM Tris, pH 8.0, 300 mM NaCl, 1 mM EDTA and 0.5% NP-40), the immunoprecipitated proteins were analyzed after SDS/PAGE by Coomassie staining or western blotting as indicated. His-UBE2J2, His-UBE2Q2, and His-UBE2D3 were incubated with 15 µl Ni-NTA agarose resin in the EBC buffer (50 mM Tris pH 7.5, 120 mM NaCl, 0.5% NP-40) supplemented with protease inhibitor (Complete Mini, Roche) for 3 hours at 4°C. Beads were washed and incubated with 3 µg HEK293T cells purified WDR24, WDR59 or Mios protein for 1 hour at 4°C. After extensively washing with low salt NETN buffer (20 mM Tris, pH 8.0, 10 mM NaCl, 1 mM EDTA and 0.5% NP-40), the immunoprecipitated proteins were analyzed after SDS/PAGE by Coomassie staining or western blotting as indicated.

In vitro Sestrin2-WDR24-UBE2D3 competition assay—GST or GST-WDR24 were incubated with Glutathione Sepharose 4B in EBC buffer for 3 hours at 4°C, and beads were washed and preloaded with the HEK-293T-purified Sestrin2 protein. After being incubated for 2 hours, the beads were extensively washed and incubated with 1 µg UBE2D3. The immunoprecipitated UBE2D3 and Sestrin2 were analyzed via immunoblotting with the

indicated antibodies. HA-WDR24 and Flag-Sestrin2 wild-type or L261A mutant were stably expressed in Sestrin13 triple null HEK293T cells, and the indicated cells were starved for all amino acids for 60 mins, lysed and subjected to anti-Flag immunoprecipitation. The immunoprecipitated GATOR2-Sestrin2 complex immobilized on HA beads was washed 3 times and then incubated with 100 μ M leucine for 20 mins in the cytosolic buffer (0.1% Triton, 40 mM HEPES pH 7.4, 10 mM NaCl, 150 mM KCl, 2.5 mM MgCl₂). Beads were washed and incubated with 1 μ g UBE2D3 for 1 hour. After washing with low salt NETN buffer (20 mM Tris, pH 8.0, 10 mM NaCl, 1 mM EDTA and 0.5% NP-40), the amount of GATOR2, Sestrin2 and UBE2D3 were analyzed via immunoblotting with the indicated antibody.

NanoBit protein-protein (PPI) assay—100ng N-Myc-LgBit-Mios Ring (Lg-Mios Ring) were co-transfected with 100ng c-SmBit-HA fused construct (WDR24 Ring-SM or WDR59 Ring-SM), c-SmBit-HA-pcDNA3.1 was used as a negative control according to the manufacturer's protocol (Promega). Twenty-four hours post-transfection, cells were plated into 96 wells (5×10^3) per well. Sixteen hours after passage, medium was removed and replaced with 100 μ l Opti-MEM medium and incubated for 1 h at 37 °C. The Nano-Glo reagent was added to each well immediately according to the manufacturer's instruction and subjected to luminescence reading. The luminescence was read every 1 min, and for the quantitative comparison of LgBit-SmBit interactions, the peak at 4 min was used.

Embryo images and histological analysis—Embryos at different days of embryonic development were collected and images with an Olympus SZ61 microscope. Embryos were subsequently fixed in 4% paraformaldehyde; 4 μ m sections were stained with hematoxylin and eosin, pS6S235/236 (CST#2211 1:100) and cleaved caspase 3 (Asp175) (CST#9661, 1:100) according to the standard procedure. Images were acquired on a Nikon Eclipse E100 microscope. Quantification was performed on ten different fields per embryo by using Image J software.

QUANTIFICATION AND STATISTICAL ANALYSIS

All the quantification analysis was performed using GraphPad Prism 8. Details on the statistical test are presented in the figure legends. All the graphs show mean \pm SD, and two-tailed unpaired Student t-tests are presented as an indication of at least three independent experiments or biological replications. $P < 0.05$ are considered as statistically significant.

Supplementary Material

Refer to Web version on PubMed Central for supplementary material.

ACKNOWLEDGMENTS

We thank all the lab members from Dr. Wei and Dr. Xiao's lab for the critical reading and helpful suggestions. We acknowledge M.L. Valenstein, K.B. Rogala, and D.M. Sabatini for reagents, feedback, and discussion of unpublished data. The works were supported by NIH grants (*R01CA177910* and *R35CA253027* to W.W.)

References

1. Saxton RA, and Sabatini DM (2017). mTOR Signaling in Growth, Metabolism, and Disease. *Cell*. 10.1016/j.cell.2017.02.004.
2. Liu GY, and Sabatini DM (2020). mTOR at the nexus of nutrition, growth, ageing and disease. *Nat Rev Mol Cell Biol*. 10.1038/s41580-019-0199-y.
3. Ma XM, and Blenis J. (2009). Molecular mechanisms of mTOR-mediated translational control. *Nat Rev Mol Cell Biol*. 10.1038/nrm2672.
4. Mossmann D, Park S, and Hall MN (2018). mTOR signalling and cellular metabolism are mutual determinants in cancer. *Nat Rev Cancer*. 10.1038/s41568-018-0074-8.
5. Kim E, Goraksha-Hicks P, Li L, Neufeld TP, and Guan KL (2008). Regulation of TORC1 by Rag GTPases in nutrient response. *Nat Cell Biol*. 10.1038/ncb1753.
6. Sancak Y, Peterson TR, Shaul YD, Lindquist RA, Thoreen CC, Bar-Peled L, and Sabatini DM (2008). The rag GTPases bind raptor and mediate amino acid signaling to mTORC1. *Science* (1979). 10.1126/science.1157535.
7. Inoki K, Li Y, Xu T, and Guan KL (2003). Rheb GTPase is a direct target of TSC2 GAP activity and regulates mTOR signaling. *Genes Dev* 17, 1829–1834. 10.1101/gad.1110003. [PubMed: 12869586]
8. Menon S, Dibble CC, Talbott G, Hoxhaj G, Valvezan AJ, Takahashi H, Cantley LC, and Manning BD (2014). Spatial control of the TSC complex integrates insulin and nutrient regulation of mTORC1 at the lysosome. *Cell* 156, 771–785. 10.1016/j.cell.2013.11.049. [PubMed: 24529379]
9. Bar-Peled L, Schweitzer LD, Zoncu R, and Sabatini DM (2012). Ragulator is a GEF for the rag GTPases that signal amino acid levels to mTORC1. *Cell* 150, 1196–1208. 10.1016/j.cell.2012.07.032. [PubMed: 22980980]
10. Sancak Y, Bar-Peled L, Zoncu R, Markhard AL, Nada S, and Sabatini DM (2010). Ragulator-rag complex targets mTORC1 to the lysosomal surface and is necessary for its activation by amino acids. *Cell* 141, 290–303. 10.1016/j.cell.2010.02.024. [PubMed: 20381137]
11. Shen K, and Sabatini DM (2018). Ragulator and SLC38A9 activate the Rag GTPases through noncanonical GEF mechanisms. *Proc Natl Acad Sci U S A* 115, 9545–9550. 10.1073/pnas.1811727115. [PubMed: 30181260]
12. Wang S, Tsun ZY, Wolfson RL, Shen K, Wyant GA, Plovovich ME, Yuan ED, Jones TD, Chantranupong L, Comb W, et al. (2015). Lysosomal amino acid transporter SLC38A9 signals arginine sufficiency to mTORC1. *Science* (1979) 347, 188–194. 10.1126/science.1257132.
13. Rebsamen M, Pochini L, Stasyk T, de Araújo MEG, Galluccio M, Kandasamy RK, Snijder B, Fauster A, Rudashevskaya EL, Bruckner M, et al. (2015). SLC38A9 is a component of the lysosomal amino acid sensing machinery that controls mTORC1. *Nature* 519, 477–481. 10.1038/nature14107. [PubMed: 25561175]
14. Wyant GA, Abu-Remaileh M, Wolfson RL, Chen WW, Freinkman E, Danai L. v., vander Heiden MG, and Sabatini DM (2017). mTORC1 Activator SLC38A9 Is Required to Efflux Essential Amino Acids from Lysosomes and Use Protein as a Nutrient. *Cell* 171, 642–654.e12. 10.1016/j.cell.2017.09.046. [PubMed: 29053970]
15. Bar-Peled L, Chantranupong L, Cherniack AD, Chen WW, Ottina KA, Grabiner BC, Spear ED, Carter SL, Meyerson M, and Sabatini DM (2013). A tumor suppressor complex with GAP activity for the Rag GTPases that signal amino acid sufficiency to mTORC1. *Science* (1979). 10.1126/science.1232044.
16. Tsun ZY, Bar-Peled L, Chantranupong L, Zoncu R, Wang T, Kim C, Spooner E, and Sabatini DM (2013). The folliculin tumor suppressor is a GAP for the RagC/D GTPases that signal amino acid levels to mTORC1. *Mol Cell* 52, 495–505. 10.1016/j.molcel.2013.09.016. [PubMed: 24095279]
17. Wolfson RL, Chantranupong L, Wyant GA, Gu X, Orozco JM, Shen K, Condon KJ, Petri S, Kedar J, Scaria SM, et al. (2017). KICSTOR recruits GATOR1 to the lysosome and is necessary for nutrients to regulate mTORC1. *Nature*. 10.1038/nature21423.
18. Peng M, Yin N, and Li MO (2017). SIRT2 dictates GATOR control of mTORC1 signalling. *Nature*. 10.1038/nature21378.

19. Valenstein ML, Rogala KB, Lalgudi P. v., Brignole EJ, Gu X, Saxton RA, Chantranupong L, Kolibius J, Quast JP, and Sabatini DM (2022). Structure of the nutrient-sensing hub GATOR2. *Nature* 607, 610–616. 10.1038/s41586-022-04939-z. [PubMed: 35831510]
20. Chantranupong L, Scaria SM, Saxton RA, Gygi MP, Shen K, Wyant GA, Wang T, Harper JW, Gygi SP, and Sabatini DM (2016). The CASTOR Proteins Are Arginine Sensors for the mTORC1 Pathway. *Cell*. 10.1016/j.cell.2016.02.035.
21. Wolfson RL, Chantranupong L, Saxton RA, Shen K, Scaria SM, Cantor JR, and Sabatini DM (2016). Sestrin2 is a leucine sensor for the mTORC1 pathway. *Science* (1979). 10.1126/science.aab2674.
22. Chen J, Ou Y, Luo R, Wang J, Wang D, Guan J, Li Y, Xia P, Chen PR, and Liu Y. (2021). SAR1B senses leucine levels to regulate mTORC1 signalling. *Nature* 596, 281–284. 10.1038/s41586-021-03768-w. [PubMed: 34290409]
23. Shen K, Huang RK, Brignole EJ, Condon KJ, Valenstein ML, Chantranupong L, Bomaliyamu A, Choe A, Hong C, Yu Z, et al. (2018). Architecture of the human GATOR1 and GATOR1-Rag GTPases complexes. *Nature*. 10.1038/nature26158.
24. Shen K, Valenstein ML, Gu X, and Sabatini DM (2019). Arg-78 of Npr12 catalyzes GATOR1-stimulated GTP hydrolysis by the Rag GTPases. *Journal of Biological Chemistry*. 10.1074/jbc.AC119.007382.
25. Dokudovskaya S, and Rout MP (2015). SEA you later alli-GATOR - A dynamic regulator of the TORC1 stress response pathway. *J Cell Sci* 128, 2219–2228. 10.1242/jcs.168922. [PubMed: 25934700]
26. Hesketh GG, Papazotos F, Pawling J, Rajendran D, Knight JDR, Martinez S, Taipale M, Schramek D, Dennis JW, and Gingras AC (2020). The GATOR-Rag GTPase pathway inhibits mTORC1 activation by lysosome-derived amino acids. *Science* (1979) 370, 351–356. 10.1126/science.aaz0863.
27. Deshaies RJ, and Joazeiro CAP (2009). RING domain E3 ubiquitin ligases. *Annu Rev Biochem*. 10.1146/annurev.biochem.78.101807.093809.
28. Joazeiro CAP, and Weissman AM (2000). RING finger proteins: Mediators of ubiquitin ligase activity. *Cell*. 10.1016/S0092-8674(00)00077-5.
29. Lipkowitz S, and Weissman AM (2011). RINGs of good and evil: RING finger ubiquitin ligases at the crossroads of tumour suppression and oncogenesis. *Nat Rev Cancer*. 10.1038/nrc3120.
30. Metzger MB, Pruneda JN, Klevit RE, and Weissman AM (2014). RING-type E3 ligases: Master manipulators of E2 ubiquitin-conjugating enzymes and ubiquitination. *Biochim Biophys Acta Mol Cell Res*. 10.1016/j.bbamcr.2013.05.026.
31. Zheng N, Schulman BA, Song L, Miller JJ, Jeffrey PD, Wang P, Chu C, Koepp DM, Elledge SJ, Paganok M, et al. (2002). Structure of the Cul1-Rbx1-Skp1-F box Skp2 SCF ubiquitin ligase complex.
32. Cardozo T, and Pagano M. (2004). The SCF ubiquitin ligase: Insights into a molecular machine. *Nat Rev Mol Cell Biol* 5, 739–751. 10.1038/nrm1471. [PubMed: 15340381]
33. Segala G, Bennesch MA, Ghahhari NM, Pandey DP, Echeverria PC, Karch F, Maeda RK, and Picard D. (2019). Vps11 and Vps18 of Vps-C membrane traffic complexes are E3 ubiquitin ligases and fine-tune signalling. *Nat Commun* 10. 10.1038/s41467-019-09800-y.
34. Yogosawa S, Hatakeyama S, Nakayama KI, Miyoshi H, Kohsaka S, and Akazawa C. (2005). Ubiquitylation and degradation of serum-inducible kinase by hVPS18, a RING-H2 type ubiquitin ligase. *Journal of Biological Chemistry* 280, 41619–41627. 10.1074/jbc.M508397200. [PubMed: 16203730]
35. Petroski MD, and Deshaies RJ (2005). Function and regulation of cullin-RING ubiquitin ligases. *Nat Rev Mol Cell Biol*. 10.1038/nrm1547.
36. Kim DH, Sarbassov DD, Ali SM, King JE, Latek RR, Erdjument-Bromage H, Tempst P, and Sabatini DM (2002). mTOR interacts with raptor to form a nutrient-sensitive complex that signals to the cell growth machinery. *Cell* 110, 163–175. 10.1016/S0092-8674(02)00808-5. [PubMed: 12150925]

37. Xu D, Zhao H, Jin M, Zhu H, Shan B, Geng J, Dziedzic SA, Amin P, Mifflin L, Naito MG, et al. (2020). Modulating TRADD to restore cellular homeostasis and inhibit apoptosis. *Nature* 587, 133–138. 10.1038/s41586-020-2757-z. [PubMed: 32968279]
38. Metzger MB, Pruneda JN, Klevit RE, and Weissman AM (2014). RING-type E3 ligases: Master manipulators of E2 ubiquitin-conjugating enzymes and ubiquitination. *Biochim Biophys Acta Mol Cell Res* 1843, 47–60. 10.1016/j.bbamcr.2013.05.026.
39. Liu J, Wang Y, Gong Y, Fu T, Hu S, Zhou Z, and Pan L. (2017). Structural Insights into SHARPIN-Mediated Activation of HOIP for the Linear Ubiquitin Chain Assembly. *Cell Rep* 21, 27–36. 10.1016/j.celrep.2017.09.031. [PubMed: 28978479]
40. Peltzer N, Darding M, Montinaro A, Draber P, Draberova H, Kupka S, Rieser E, Fisher A, Hutchinson C, Taraborrelli L, et al. (2018). LUBAC is essential for embryogenesis by preventing cell death and enabling haematopoiesis. *Nature* 557, 112–117. 10.1038/s41586-018-0064-8. [PubMed: 29695863]
41. Akimov V, Barrio-Hernandez I, Hansen SVF, Hallenborg P, Pedersen AK, BekkerJensen DB, Puglia M, Christensen SDK, Vanselow JT, Nielsen MM, et al. (2018). Ubisite approach for comprehensive mapping of lysine and n-terminal ubiquitination sites. *Nat Struct Mol Biol* 25, 631–640. 10.1038/s41594-018-0084-y. [PubMed: 29967540]
42. Udeshi ND, Svinkina T, Mertins P, Kuhn E, Mani DR, Qiao JW, and Carr SA (2013). Refined preparation and use of anti-diglycine remnant (k-e-gg) antibody enables routine quantification of 10,000s of ubiquitination sites in single proteomics experiments. *Molecular and Cellular Proteomics* 12, 825–831. 10.1074/mcp.O112.027094. [PubMed: 23266961]
43. Kim W, Bennett EJ, Huttlin EL, Guo A, Li J, Possemato A, Sowa ME, Rad R, Rush J, Comb MJ, et al. (2011). Systematic and quantitative assessment of the ubiquitin-modified proteome. *Mol Cell* 44, 325–340. 10.1016/j.molcel.2011.08.025. [PubMed: 21906983]
44. Kostrhon S, Prabu JR, Baek K, Horn-Ghetko D, von Gronau S, Klügel M, Basquin J, Alpi AF, and Schulman BA (2021). CUL5-ARIH2 E3-E3 ubiquitin ligase structure reveals cullin-specific NEDD8 activation. *Nat Chem Biol* 17, 1075–1083. 10.1038/s41589-021-00858-8. [PubMed: 34518685]
45. Harper JW, and Schulman BA (2021). Cullin-RING Ubiquitin Ligase Regulatory Circuits: A Quarter Century beyond the F-Box Hypothesis. *Annu Rev Biochem* 90, 403–429. 10.1146/annurev-biochem-090120-013613. [PubMed: 33823649]
46. Petroski MD, and Deshaies RJ (2005). Function and regulation of cullin-RING ubiquitin ligases. *Nat Rev Mol Cell Biol* 6, 9–20. 10.1038/nrm1547. [PubMed: 15688063]
47. Novellasdemunt L, Kucharska A, Jamieson C, Prange-Barczynska M, Baulies A, Antas P, van der Vaart J, Gehart H, Maurice MM, and Li VS (2020). NEDD4 and NEDD4L regulate Wnt signalling and intestinal stem cell priming by degrading LGR5 receptor. *EMBO J* 39. 10.15252/embj.2019102771.
48. Anan T, Nagata Y, Koga H, Honda Y, Yabuki N, Miyamoto C, Kuwano A, Matsuda I, Endo F, Saya H, et al. (1998). Human ubiquitin-protein ligase Nedd4: Expression, subcellular localization and selective interaction with ubiquitin-conjugating enzymes. *Genes to Cells* 3, 751–763. 10.1046/j.1365-2443.1998.00227.x. [PubMed: 9990509]
49. Efeyan A, Schweitzer LD, Bilate AM, Chang S, Kirak O, Lamming DW, and Sabatini DM (2014). RagA, but Not RagB, Is Essential for Embryonic Development and Adult Mice. *Dev Cell* 29, 321–329. 10.1016/j.devcel.2014.03.017. [PubMed: 24768164]
50. Narita T, Weinert BT, and Choudhary C. Functions and mechanisms of non-histone protein acetylation. *Nat Rev Mol Cell Biol*. 10.1038/s41580.
51. Celen AB, and Sahin U. (2020). Sumoylation on its 25th anniversary: mechanisms, pathology, and emerging concepts. *FEBS Journal* 287, 3110–3140. 10.1111/febs.15319. [PubMed: 32255256]
52. Murn J, and Shi Y. (2017). The winding path of protein methylation research: Milestones and new frontiers. *Nat Rev Mol Cell Biol* 18, 517–527. 10.1038/nrm.2017.35. [PubMed: 28512349]

Highlights

- Ring disruption in Mios, WDR24 and WDR59 impedes AA-mediated mTORC1 activation
- Mios functions as a brake to prevent the self-ubiquitination of WDR24
- Leucine dissociates Sestrin2 from WDR24 Ring, leading to NPRL2 ubiquitination
- *Wdr24* deficiency prevents mTORC1 activation, leading to embryonic lethality in mice

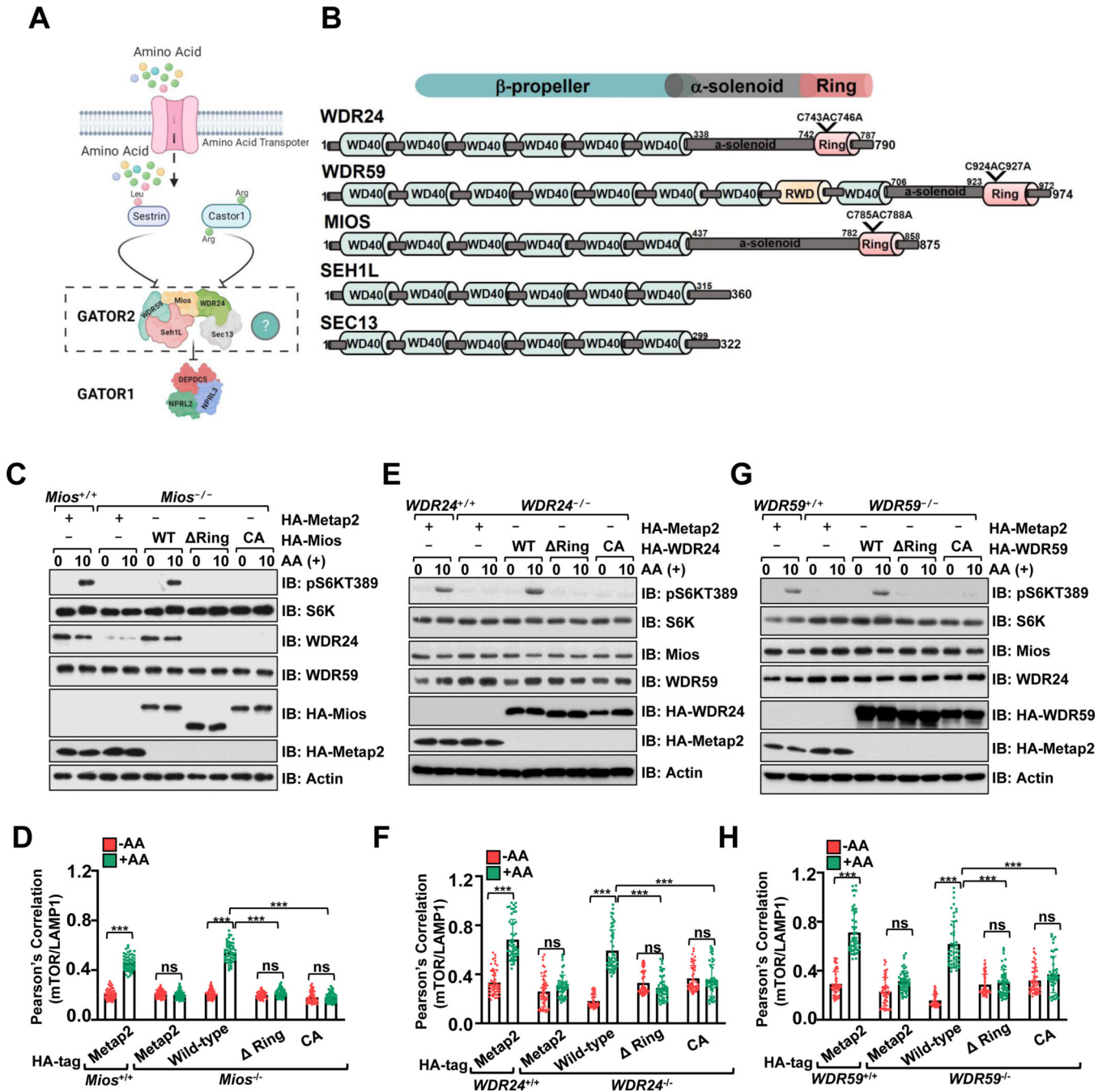


Figure 1. The Ring domains are critical for GATOR2 to transmit amino acid availability to mTORC1.

A. Model depicting how GATOR2 acts as a hub to timely sense the cytosolic amino acids.

B. A schematic illustration of the annotated domains of GATOR2 components.

C. Wild-type or *Mios* knockout HEK 293 cells were infected with indicated constructs. The resulting cells were deprived of amino acids for 60 min and restimulated with amino acids for 10 min. Whole cell lysates were analyzed via immunoblotting by probing with indicated antibodies. Metap2 was used as a negative control.

D. Cells were treated as in (C), and the co-localization of mTORC1 and LAMP1 was analyzed via immuno-staining. The imaging data were quantified with 50 cells under each condition. Data are mean \pm SD, two-tailed t-test. ns, no significance, *** $P < 0.001$. See Figure S1M for imaging data.

E. Wild-type or *WDR24* knockout HEK 293 cells were infected with indicated constructs. The resulting cells were deprived of amino acids for 60 min and restimulated with amino acids for 10 min. Whole cell lysates were analyzed via immunoblotting by probing with indicated antibodies.

F. Cells were treated as in (E). The co-localization of mTORC1 and LAMP1 was analyzed via immuno-staining. The imaging data were quantified with 50 cells under each condition. Data are mean \pm SD, two-tailed t-test. ns, no significance, *** $P < 0.001$. See Figure S1N for imaging data.

G. Wild-type or *WDR59* knockout HEK 293 cells were infected with indicated constructs. The resulting cells were deprived of amino acids for 60 min and restimulated with amino acids for 10 min. Whole cell lysates were analyzed via immunoblotting by probing with indicated antibodies.

H. Cells were treated as in (G). The co-localization of mTORC1 and LAMP1 was analyzed via immuno-staining. The imaging data were quantified with 50 cells under each condition. Data are mean \pm SD, two-tailed t-test. ns, no significance, *** $P < 0.001$. See Figure S1O for imaging data.

See also Figure S1

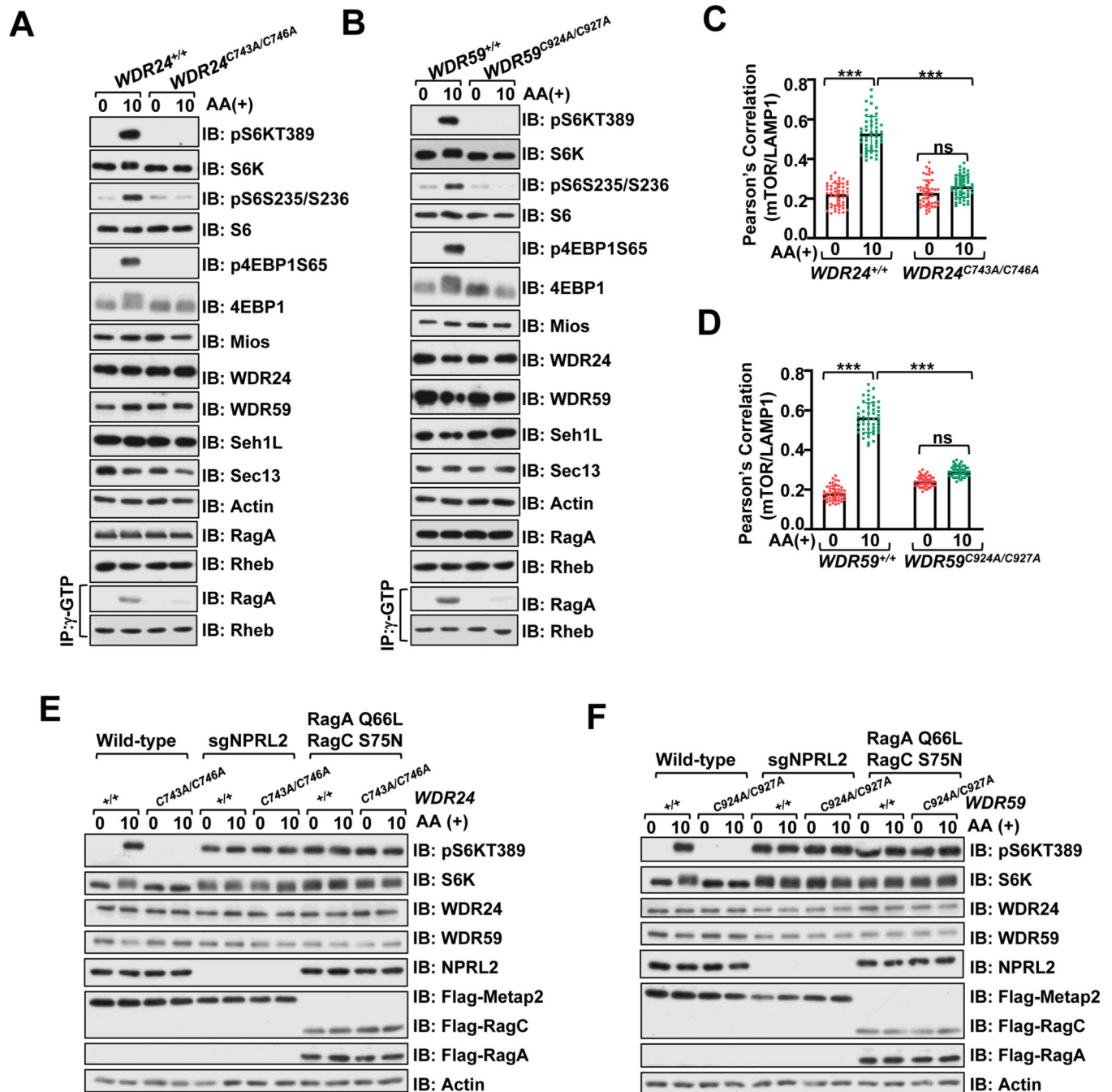


Figure 2. Genetic mutation of the core residues in WDR24 or WDR59 Ring domain impairs amino acid-mediated mTORC1 activation.

A. Wild-type or *WDR24*^{C743A/746A} knock-in HEK 293 cells were deprived of amino acids for 60 min and stimulated with amino acids for 10 min. Cells were lysed and analyzed by immunoblotting with indicated antibodies.

B. Wild-type or *WDR59*^{C924A/927A} knock-in HEK 293 cells were deprived of amino acids for 60 min and stimulated with amino acids for 10 min. Cells were lysed and analyzed by immunoblotting with indicated antibodies.

C. Cells were treated as in (A), and the co-localization of mTORC1 and LAMP1 was analyzed via immuno-staining . Scale bar, 10 μ m. The imaging data were quantified with 50 cells under each condition. Data are mean \pm SD, two-tailed t-test. ns, no significance, ***P < 0.001. See Figure S2G for imaging data.

D. Cells were treated as in (B), and the co-localization of mTORC1 and LAMP1 was analyzed via immuno-staining. Scale bar, 10 μ m. The imaging data were quantified with 50 cells under each condition. Data are mean \pm SD, two-tailed t-test. ns, no significance, ***P < 0.001. See Figure S2H for imaging data.

E-F. Indicated cells were infected with *sgNPRL2* or lentivirus expressing the RagAQ66L (E) or RagCS75N transgenes (F). Cells were deprived of amino acids for 60 min and stimulated with amino acids for 10 min. Cells were lysed and analyzed by immunoblotting with indicated antibodies. Metap2 was used as a negative control.

See also Figure S2

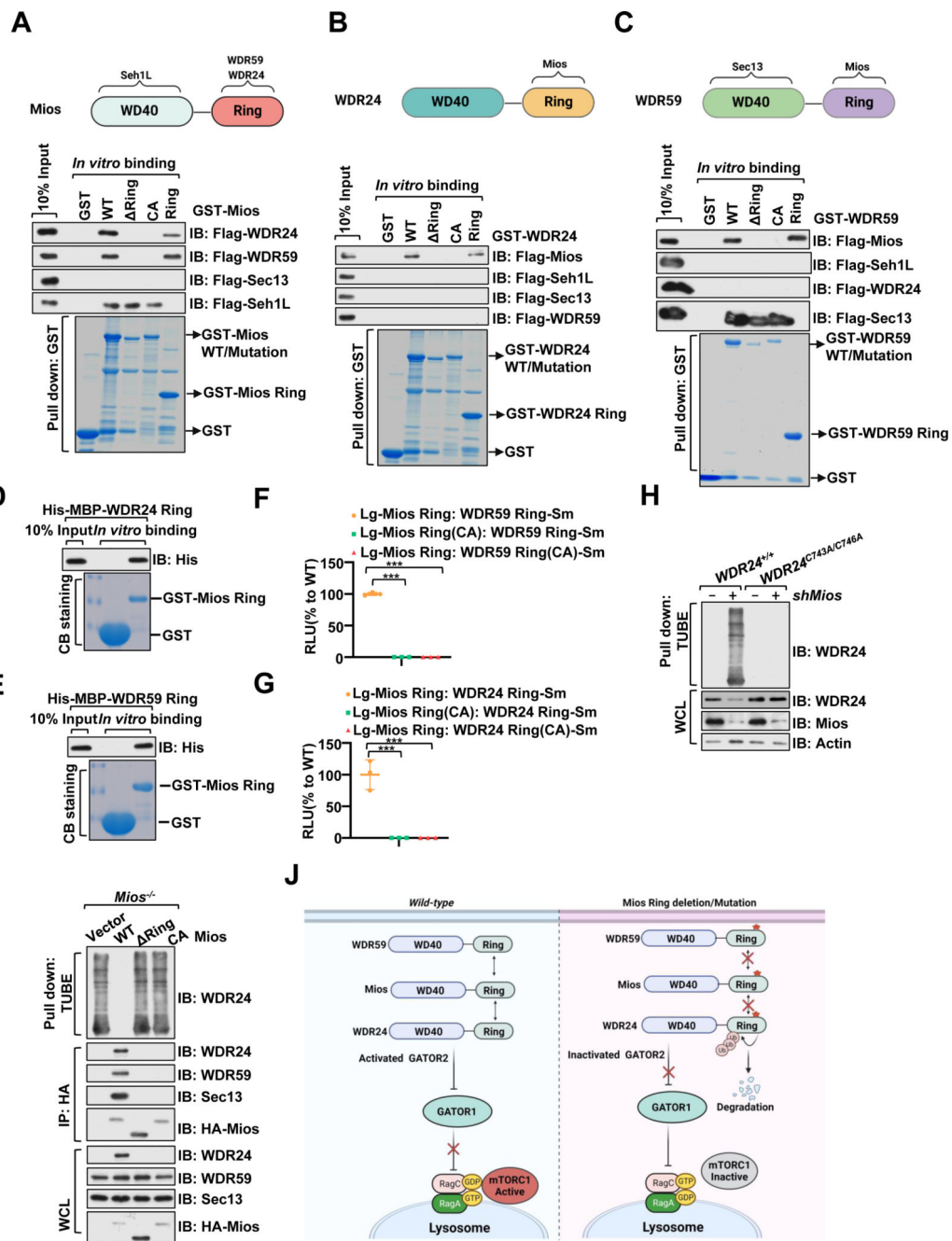


Figure 3. Ring domains are critical for intra-molecular interaction of Mios, WDR24 and WDR59 within the GATOR2 complex.

A. Immunoblot analysis from the pull-down assay using GST-Mios wild-type, Ring, CA, Ring deletion fragments immobilized on GST affinity beads and incubated with other purified subunits from HEK293T cells.

B. Immunoblot analysis from the pull-down assay using GST-WDR24 wild-type, Ring, CA, Ring deletion fragments immobilized on GST affinity beads and incubated with other purified subunits from HEK293T cells.

C. Immunoblot analysis from the pull-down assay using GST-Mios wild-type, Ring, CA, Ring deletion fragments immobilized on GST affinity beads and incubated with other purified subunits from HEK293T cells.

D-E. Immunoblot analysis from pull-down assay using tandem GST, GST-Mios Ring domain with the recombinant His-MBP-WDR24 Ring (D) and His-MBP-WDR59 Ring (E).

F-G. Mutation of conserved cysteine residues in the Ring domains of Mios, WDR24, and WDR59 dramatically reduced the interaction of the intra-molecular binding affinity of Mios Ring-WDR24 Ring (F) and Mios Ring-WDR59 Ring domain (G). Quantitative comparison of LgBit-SmBit interactions. The peak at 4 min was used. Data are mean \pm SD (n=3), two-tailed t-test. ns, no significance, ***P < 0.001.

H. TUBE (tandem ubiquitin-binding entity) pulled down the ubiquitinated WDR24 from the indicated cells.

I. The interaction of Mios wild type, Ring, and CA mutants with other subunits was analyzed using an immunoprecipitated assay. The ubiquitination level of WDR24 was analyzed via TUBE-pull down assay.

J. A schematic illustration of the Ring domains of GATOR2 in mediating intramolecular interaction to govern its function in amino acid-dependent activation of mTORC1. See also Figure S3.

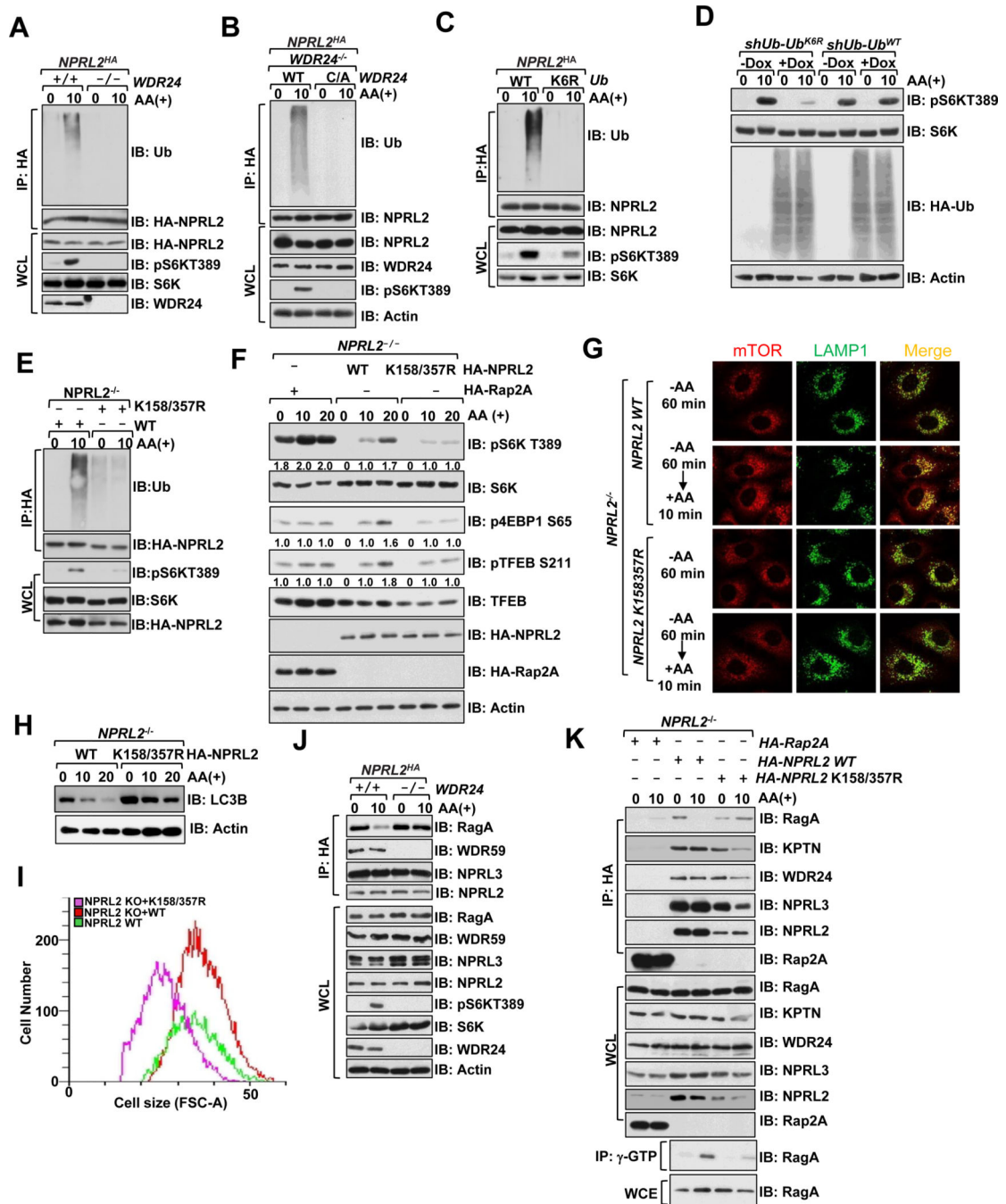


Figure 4. WDR24 has intrinsic E3 ubiquitin ligase activity.

A. Depletion of *WDR24* abolishes amino acid-induced ubiquitination of NPRL2. *NPRL2^{HA}* HEK293 cells with or without *CRISPR-Cas9-mediated WDR24* knockout were deprived of amino acids for 60 min or starved and restimulated with amino acids for 10 min. Cells lysis were immunoprecipitated with HA beads under denatured condition and probed with indicated antibodies.

B. *WDR24^{-/-}* in *NPRL2^{HA}* background were reconstituted with *WDR24 wild-type* or *WDR24^{C743A/746A}* mutants. The ubiquitination level of NPRL2 was analyzed as in (A).

C. K6R Ub mutant was transfected into *NPRL2^{Flag}* knock-in cells, and the ubiquitination of NPRL2 was analyzed via immunoblotting.

D. The indicated cells were treated with doxycycline (100 ng/ml) for 12 hours. The doxycycline-induced cells were starved with amino acids for 60 mins and restimulated with amino acids for 10 mins. Cells were lysed and analyzed via immunoblotting with the indicated antibody.

E. The K157/358R mutation prevents NPRL2 ubiquitination.

F. Immunoblotting analysis of WCL derived from *NPRL2* knockout HeLa cells infected with wild-type and K158/357R mutant. Cells were deprived of amino acids for 60 mins and restimulated with amino acids for 10 or 20 min before harvesting immunoblotting with indicated antibodies. The quantification with phosphorylation status of mTORC1 substrates were analyzed via Image J.

G. Cells were starved as in (F) and then restimulated with amino acid for 20 mins, and the co-localization of mTORC1 and LAMP1 was analyzed via immuno-staining.

H. Wild-type or *NPRL2^{K158/357R}* reconstituted *NPRL2^{-/-}* HeLa cells were starved with amino acids for 2 hours and restimulated with amino acids at the indicated time. The levels of p-S6KT389 and LCB were analyzed via immunoblotting.

I. Cell size analysis from *wild-type* or *NPRL2^{K158/357R}* reconstituted *NPRL2^{-/-}* HeLa cells by FACS.

J. *NPRL2^{HA}* HEK293 cells with or without CRISPR-Cas9-mediated WDR24 knockout were deprived of amino acids for 60 mins or starved and restimulated with amino acids for 10 mins. Cell lysis was immunoprecipitated with anti-HA beads; the immunocomplexes were analyzed by western blotting via probing with the indicated antibody.

K. Immunoblotting analysis of whole-cell lysis and anti-HA-immunoprecipitated derived from *NPRL2^{-/-}* HeLa cells reconstituted with different constructs. Cells were deprived of amino acids for 60 mins and restimulated with amino acids for 10 mins before harvesting for immunoprecipitation and immunoblotting analyses.

See also Figure S4.

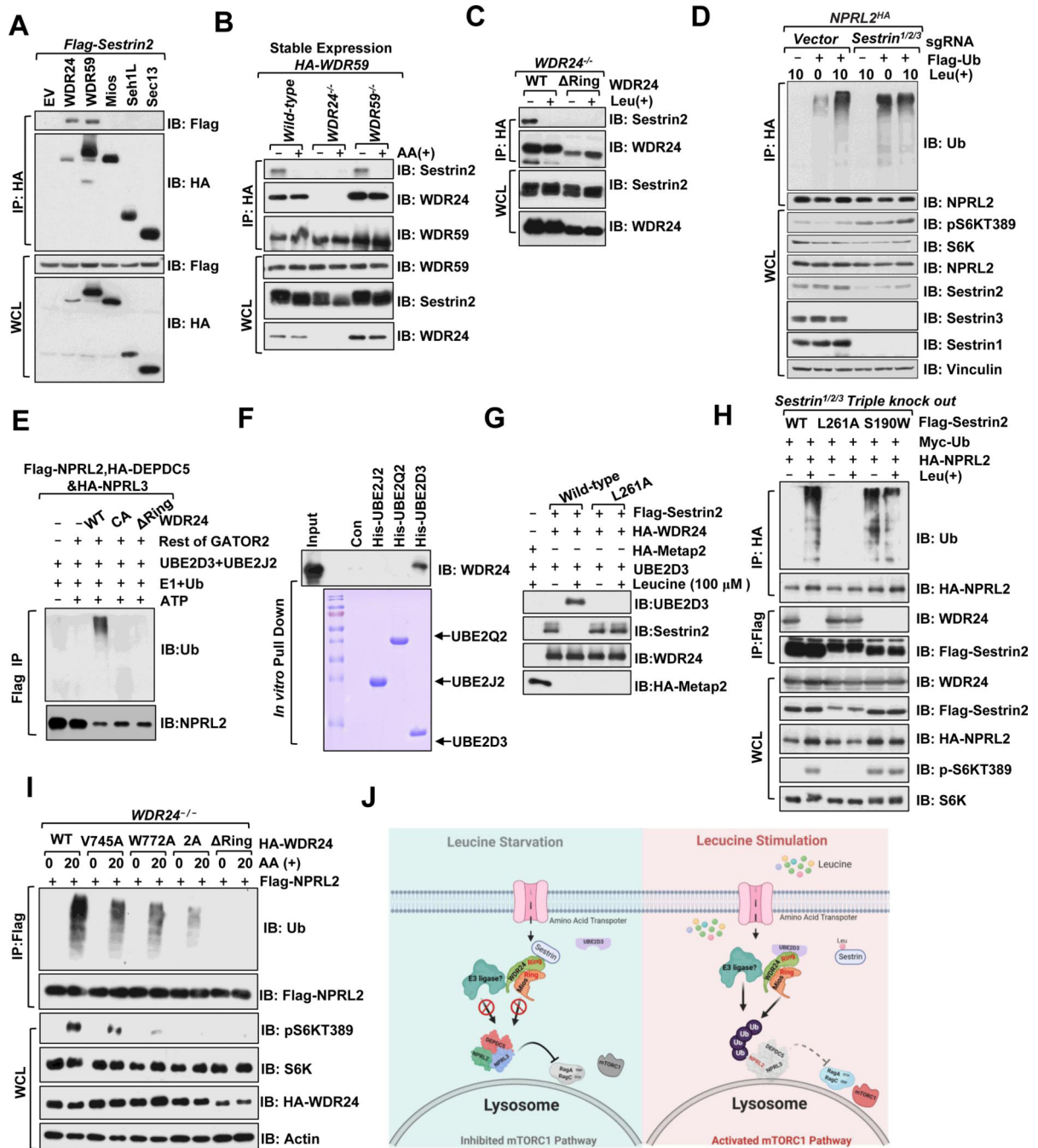


Figure 5. Ring domain of WDR24 is essential for its interaction with Sestrin2.

A. Flag-Sestrin2 was co-transfected with HA-WDR24, HA-WDR59, HA-Mios, HA-Seh1L, and HA-Sec13 in HEK293T cells. Cells were lysed and immunoprecipitated with HA beads, and the immunocomplexes were analyzed by immunoblotting as indicated.

B. *Wild-type*, *WDR24*^{-/-} and *WDR59*^{-/-} cells were infected with HA-WDR59 constructs. The resulting cells were lysed and immunoprecipitated with HA beads, and the immunocomplexes were analyzed by immunoblotting with indicated antibodies.

C. *WDR24*^{-/-} cells were infected with HA-WDR24 wild-type and Ring constructs. Cells were lysed and immunoprecipitated with HA beads, and the immunocomplexes were analyzed by immunoblotting with indicated antibodies.

D. The *NPRL2*^{HA} knock-in HEK 293 cells were first infected with lentiviral constructs expressing Cas9-sgSESN1/2/3. Infected cells were selected with 1 µg/ml puromycin for 72 hours to eliminate the non-infected cells. The resulting cells were deprived of leucine for 60 mins or starved and restimulated with leucine for 10 mins before harvesting for IP and IB analyses.

E. *In vitro* poly-ubiquitination of *NPRL2* by *in vitro* reconstituted GATOR2 (from recombinant proteins).

F. Binding assay among different E2 enzymes with WDR24. 5 µg His6-tag E2 enzymes were immobilized on Ni-NTA beads and were incubated with 293T purified Flag-WDR24. The interaction was analyzed by immunoblotting with the Flag-antibody.

G. Leucine restored the interaction of WDR24 with UBE2D3. HA-WDR24 and Flag-Sestrin2 or Flag-Sestrin2 L261A mutant were co-transfected into Sestrin1–3 triple-null HEK 293T cells. Cells were deprived of full amino acids for 60 min, and leucine (100 µM) was added directly to the immunoprecipitants. After re-washing, the immunocomplex was incubated with UBE2D3, and the interaction was analyzed by immunoblotting with the indicated antibody.

H. *Sestrin1–3* triple-null cells expressing Sestrin2 wild-type, L261A (do not bind to leucine), S190W (do not bind to WDR24) were infected with HA-*NPRL2* expressing virus and selected with puromycin (1 µg/mL). Cells were then transfected with Myc-Ub, and resulting cells were deprived of leucine for 60 min or starved and restimulated with leucine for 10 min. The ubiquitination of *NPRL2* was analyzed as in (D).

I. *WDR24*^{-/-} in *NPRL2*^{HA} background were reconstituted with indicated constructs. The mTORC1 activation and ubiquitination level of *NPRL2* was analyzed.

J. A schematic depicting Sestrin2 and Mios/WDR24 Ring interaction mode in response to leucine availability. Upon leucine stimulation, Sestrin2 dissociates from the Ring domain of WDR24 accompanied by WDR24-Mios Ring conformational changes, leading to a Ring-Ring semi-open status, WDR24 ubiquitinates *NPRL2*. In the status of leucine starvation, Sestrin2 and Mios bind to the Ring domain of WDR24, leading to a closed Ring-Ring interaction mode, in which the E3 activity of WDR24 is blocked. Other E3 ligase might interact with GATOR2 to dictate amino-acids mediated *NPRL2* ubiquitination.

See also Figure S5.

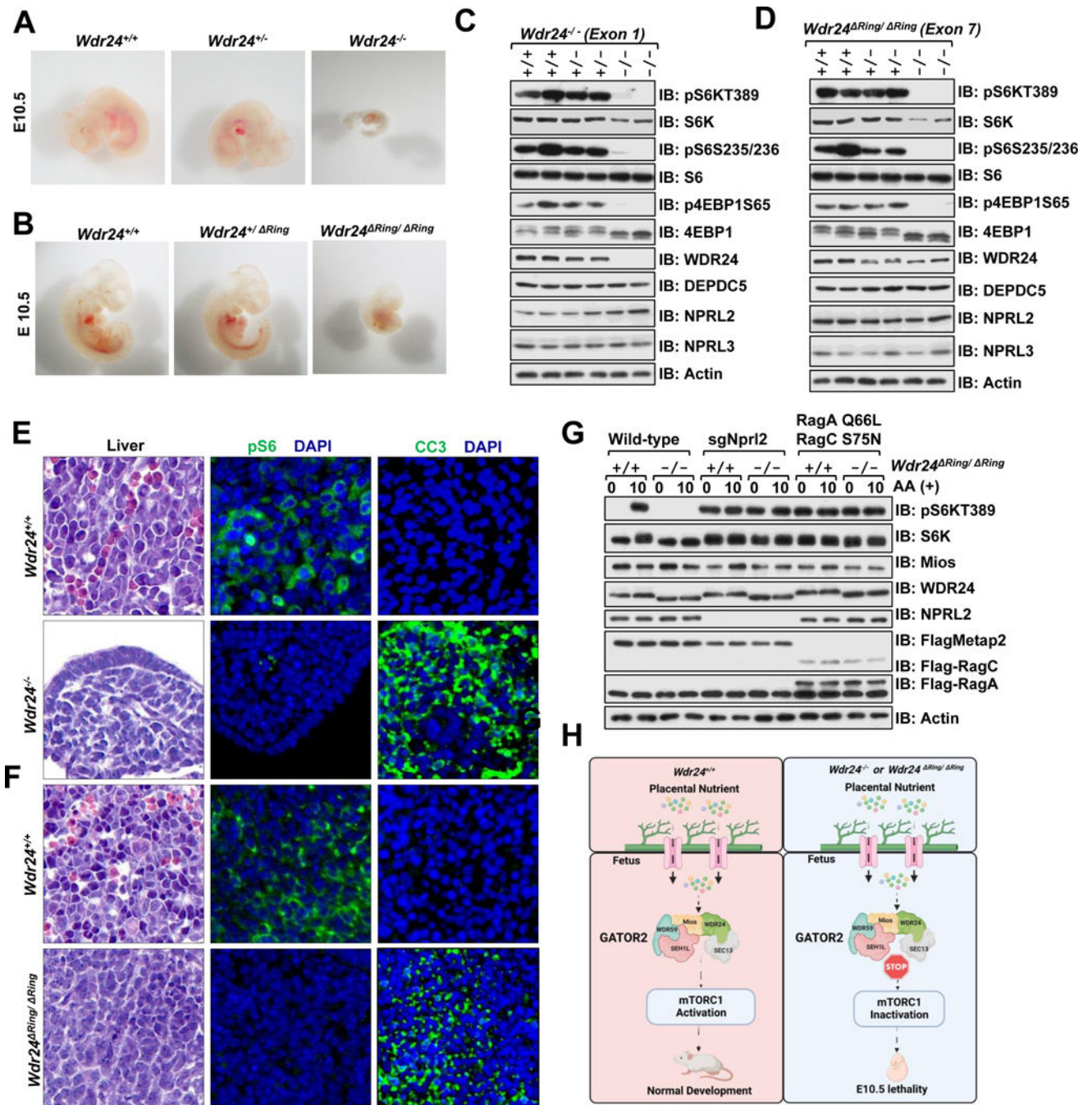


Figure 6. Wdr24 Ring domain deletion phenocopies *Wdr24* deficiency in mouse, leading to reduced mTORC1 signaling and embryonic lethality.

A. Representative images of embryos from E10.5 of *Wdr24*^{+/+}, *Wdr24*^{+/-} and *Wdr24*^{-/-} mouse embryos.

B. Representative images of embryos from E10.5 of *Wdr24*^{+/+}, *Wdr24*^{Ring/+} and *Wdr24*^{Ring/Ring} embryo.

C. Whole embryo protein extracts from *Wdr24*^{+/+}, *Wdr24*^{+/-} and *Wdr24*^{-/-} littermates were analyzed via immunoblotting with the indicated antibody.

- D.** Whole embryo protein extracts from *Wdr24^{+/+}*, *Wdr24^{Ring/+}* and *Wdr24^{Ring/Ring}* littermates were analyzed via immunoblotting with the indicated antibody.
- E.** Representative images of hematoxylin and eosin (H&E), p-S6(S235/236), CC3(cleaved-Caspase 3) staining of the liver section (n=3) of *Wdr24^{+/+}* and *Wdr24^{-/-}* littermates.
- F.** Representative images of hematoxylin and eosin (H&E), p-S6(S235/236), CC3(cleaved-Caspase 3) staining of the liver section (n=3) of *Wdr24^{+/+}* and *Wdr24^{Ring/Ring}* littermates.
- G.** *Wdr24^{+/+}* and *Wdr24^{Ring/Ring}* MEF cells were infected with sgNpr12 and lentivirus expressing the *RagA^{Q66L}* or *RagC^{S75N}* transgenes. Cells were deprived of amino acids for 60 min and stimulated with amino acids for 10 min. Cells were lysed and analyzed by immunoblotting with indicated antibodies.
- H.** A schematic illustration of the proposed role of the Ring domains of GATOR2 in amino acid-mediated mTORC1 activation during embryonic development.
See also Figure S6.

KEY RESOURCES TABLE

REAGENT or RESOURCE	SOURCE	IDENTIFIER
Antibodies		
Rabbit anti-WDR59	Cell Signaling Technology	Cat#: 53385
Rabbit anti-Mios	Cell Signaling Technology	Cat#: 13557
Rabbit anti-RagA	Cell Signaling Technology	Cat#: 4357
Rabbit anti-pS6K T389	Cell Signaling Technology	Cat#: 9234
Rabbit anti-S6K	Cell Signaling Technology	Cat#: 2708
Rabbit anti-S6	Cell Signaling Technology	Cat#: 2317
Rabbit anti-pS6 S235/236	Cell Signaling Technology	Cat#: 4858
Rabbit anti-pTFEB S211	Cell Signaling Technology	Cat#: 37681
Rabbit anti-p4EBP1 S65	Cell Signaling Technology	Cat#: 9451
Rabbit anti-4EBP1	Cell Signaling Technology	Cat#: 9644
Rabbit anti-NPRL2	Cell Signaling Technology	Cat#: 37344
Rabbit anti-Flag	Cell Signaling Technology	Cat#: 14793
Rabbit anti-HA	Cell Signaling Technology	Cat#: 3724
Rabbit anti-LC3B	Cell Signaling Technology	Cat#: 3968
Rabbit anti-mTOR	Cell Signaling Technology	Cat#: 2983
Rabbit anti-NEDD4	Cell Signaling Technology	Cat#: 2740
Rabbit anti-Rheb	Cell Signaling Technology	Cat#: 13879
Rabbit anti-WDR24	Proteintech	Cat#: 20778
Rabbit anti-SEC13	Proteintech	Cat#: 15397
Rabbit anti-TFEB	Proteintech	Cat#: 13372
Rabbit anti-Sestrin2	Proteintech	Cat#: 10795
Rabbit anti-Ubiquitin	Proteintech	Cat#: 10201
Rabbit anti- β -Actin	Proteintech	Cat#: 20536
Rabbit anti-Sestrin1	Proteintech	Cat#: 21668
Rabbit anti-Sestrin3	Proteintech	Cat#: 24532
Rabbit anti-UBE2D3	Proteintech	Cat#: 11677
Rabbit anti-UBE2J2	Proteintech	Cat#: 17713
Rabbit anti-NPRL3	Abcam	Cat#: ab121346
Rabbit anti-SEH1L	Abcam	Cat#: ab218531
Mouse anti-LAMP1	Abcam	Cat#: ab25630
Rabbit anti-DEPDC5	My-BioSource	Cat#: MBS6011892
HRP-conjugated anti-mouse secondary antibody	Sigma-Aldrich	Cat#: A-4416
HRP-conjugated anti-rabbit secondary antibody	Sigma-Aldrich	Cat#: A-4914
Anti-mouse Alexa Fluor 488	Life Technologies/ Molecular Probes	Cat#: A11001

REAGENT or RESOURCE	SOURCE	IDENTIFIER
Anti-Rabbit Alexa Fluor 594	Life Technologies/ Molecular Probes	Cat#: A32740
Bacterial and Virus Strains		
XL10 Gold Escherichia coli	Agilent	Cat #200314
BL21(DE3) Escherichia coli	Dr. William G. Kaelin, Jr., Dana-Farber Cancer Institute	N/A
E.coli: One Shot Stbl3 Chemically competent cells	Thermo Fisher Scientific	Cat#C737303
Chemicals, Peptides, and Recombinant Proteins		
Anti-FLAG M2 Affinity Gel	Sigma-Aldrich	Cat#: A-2220
Anti-HA M2 Affinity Gel	Sigma-Aldrich	Cat#: A-2095
TUBE-beads	Life Sensors	Cat#: UM502T
Flag peptide	Sigma-Aldrich	Cat#: F4799
Full Amino-acids-Deficient Medium	USBiological Life Sciences	Cat#: R8999-04A
Leucine-Deficient Medium	USBiological Life Sciences	Cat#: R8998-02
Arginine-Deficient Medium	USBiological Life Sciences	Cat#: R8998-01
Dialyzed FBS	Gibico	Cat#: 26400044
Chloroquine	Sigma	Cat#: C6628
MG-132	Enzo Life Sciences	Cat#: BML-PI102
Experimental Models: Cell Lines		
HEK293	Dr. William G. Kaelin, Jr., Dana-Farber Cancer Institute	N/A
HEK293T	Dr. William G. Kaelin, Jr., Dana-Farber Cancer Institute	N/A
<i>NPRL2^{Flag}</i> HEK293T cells	Dr. David M. Sabatini Whitehead Institute	N/A
<i>Sestrin1/2/3</i> triple knockout HEK293T cells	Dr. David M. Sabatini Whitehead Institute	Rachel et al., 2016
shUb-Ub ^{K6R} -Reconstituted U2OS cells	Dr. Zhijian James Chen UT Southwestern	Ming et al., 2009
shUb-Ub ^{wild-type} Reconstituted U2OS cells	Dr. Zhijian James Chen UT Southwestern	Ming et al., 2009
Experimental Models: Organisms/Strains		
C57BL/6	Shanghai Laboratory Animal Center	N/A
Recombinant DNA		
PGEX-GST-6p-2-Mios Wild-type	This paper	N/A
PGEX-GST-6p-2-Mios Ring (1-784)	This paper	N/A
PGEX-GST-6p-2-Mios ^{C785A/C788A}	This paper	N/A
PGEX-GST-6p-2-Mios Ring (785-875)	This paper	N/A
PGEX-GST-WDR59 Wild-type	This paper	N/A
PGEX-GST-WDR59 Ring (1-923)	This paper	N/A
PGEX-GST-WDR59 ^{C924A/C927A}	This paper	N/A

REAGENT or RESOURCE	SOURCE	IDENTIFIER
His-MBP-WDR59 Ring (924–974)	This paper	N/A
PGEX-GST-6p-2-WDR24 Wild-type	This paper	N/A
PGEX-GST-6p-2-WDR24 Ring (1–742)	This paper	N/A
PGEX-GST-6p-2-WDR24 ^{C743A/C746A}	This paper	N/A
His-MBP-WDR24 Ring (743–790)	This paper	N/A
Flag-WDR59-pRK5	This paper	N/A
Flag-Sec13-pRK5	This paper	N/A
Flag-Seh1L-pRK5	This paper	N/A
Flag-WDR24-pRK5	Bar-Peled et al. 2013	Addgene 46334
C terminal-Flag-Mios-pRK5	Bar-Peled et al. 2013	Addgene 46326
C terminal-HA-Mios pRK5	Bar-Peled et al. 2013	Addgene 46329
HA-WDR24-pRK5	Bar-Peled et al. 2013	Addgene 46335
C terminal-HA-WDR59-pRK5	Bar-Peled et al. 2013	Addgene 46328
HA-Sec13-pRK5	Bar-Peled et al. 2013	Addgene 46332
HA-Seh1L-pRK5	Bar-Peled et al. 2013	Addgene 46331
pLVX-CMV-HA-Mios Wild-type	This paper	N/A
pLVX-CMV-HA-Mios Ring (1–784)	This paper	N/A
pLVX-CMV-HA-Mios ^{C785A/C788A}	This paper	N/A
pLVX-CMV-HA-Mios WD40 (438–875)	This paper	N/A
pLVX-CMV-HA-WDR59 Wild-type	This paper	N/A
pLVX-CMV-HA-WDR59 Ring (1–923)	This paper	N/A
pLVX-CMV-HA-WDR59 ^{C924A/C927A}	This paper	N/A
pLVX-CMV-HA-WDR59 WD40-1(363–974)	This paper	N/A
pLVX-CMV-HA-WDR59 WD40-2(707–974)	This paper	N/A
pLVX-CMV-HA-WDR24 Wild-type	This paper	N/A
pLVX-CMV-HA-WDR24 Ring (1–742)	This paper	N/A
pLVX-CMV-HA-WDR24 ^{C743A/C746A}	This paper	N/A
pLVX-CMV-HA-WDR24 WD40(339–790)	This paper	N/A
Flag-NPRL2-pRK5	Bar-Peled et al. 2013	Addgene 46333
HA-NPRL3-pRK5	Bar-Peled et al. 2013	Addgene 46330
HA-DEPDC5-pRK5	Bar-Peled et al. 2013	Addgene 46327
pLVX-CMV-HA-NPRL2 K158/357R	This paper	N/A
pLVX-CMV-HA-NPRL2	This paper	N/A
pRK5 CASTOR1-Flag Cterm	Chantranupong et al.2016	Addgene 84488
pRK5-FLAG-Sestrin2	Chantranupong et al.2014	Addgene 72595
pRK5-FLAG-Sestrin2 S190W	Wolfson et al. 2016	Addgene 73670
pRK5-FLAG-Sestrin2 L261A	Wolfson et al. 2016	Addgene 73671

REAGENT or RESOURCE	SOURCE	IDENTIFIER
N-Myc-LgBiT-pcDNA3.1-Mios Ring(785–875)	This paper	N/A
c-SmBit-HA-pcDNA3.1-WDR24 Ring(743–790)	This paper	N/A
c-SmBit-HA-pcDNA3.1-WDR59 Ring(924–974)	This paper	N/A
N-Myc-LgBiT-pcDNA3.1-Mios Ring ^{C785A/C788A}	This paper	N/A
c-SmBit-HA-pcDNA3.1-WDR24 Ring ^{C743A/C746A}	This paper	N/A
c-SmBit-HA-pcDNA3.1-WDR59 Ring ^{C924A/C927A}	This paper	N/A
pLVX-CMV-HA-WDR24 ^{V745A}	This paper	N/A
pLVX-CMV-HA-WDR24 ^{V745D}	This paper	N/A
pLVX-CMV-HA-WDR24 ^{W772A}	This paper	N/A
pLVX-CMV-HA-WDR24 ^{W772D}	This paper	N/A
pLVX-CMV-HA-WDR24 ^{V745A/W772A}	This paper	N/A
pLVX-CMV-HA-WDR24 ^{V745D/W772D}	This paper	N/A
CMV-GST-WDR24 Ring-1(601–790)	This paper	N/A
CMV-GST-WDR24 Ring-2(701–790)	This paper	N/A
Oligonucleotides		
<i>NPRL2</i> ^{HA} knock-in cell line	sg <i>NPRL2</i> - F:caccgGATGCGGCAGCC GCTGCCCA sg <i>NPRL2</i> - R:aaacTGGGCAGCGGCT GCCGCATC	N/A
<i>NPRL2</i> ^{HA} knock-in cell line	SSODN: CGAGGAACGAGGAGCT ACGGCCTGGGCC CGTTATTGCCATGTACC CATACGATGTTT CAGATTACGCTGGCTAT CCCTATGACGTCC CGGACTATGCAGGATAT CCATATGACGTTT CAGATTACGCTGGTGGC GGAGGATCCGGGT CCGGGTGTAGGATAGAA TGCATATTCTTCA GCGAGTTCCACCCACG CTGGGAC	N/A
<i>NPRL2</i> ^{HA} knock-in cell line validation	<i>NPRL2</i> -1F: AGCCACGCCTCTGAGTC <i>NPRL2</i> -1R: CTCTAGCCTC ACAGTTGTC	N/A
<i>NPRL3</i> ^{Flag} knock-in cell line	sg <i>NPRL3</i> - F:caccgTGTGTCCCGCAT CCCGCCG sg <i>NPRL3</i> - R:aaacCGGCGGGATGCG GGACAACAc	N/A

REAGENT or RESOURCE	SOURCE	IDENTIFIER
<i>NPRL3^{Flag}</i> knock-in cell line	SSODN: GTCTCCTCTGGCCCC TCCGCCCCGGCC CCGGCCCCACGGCGG ATGGACTACAAAG ACCATGACGGTGATTAT AAAGATCATGACA TTGATTACAAGGATGAC GATGACAAGGCG GCCGCAGGCAGGGATAA TACTAGCCCCATC AGCGTGATTCTGGTGAG CTCGGGGAGCAG GGCAATAAG	N/A
<i>NPRL3^{Flag}</i> knock-in cell line validation	<i>NPRL3</i> -F: CCTGCCCTCCTCAGGC <i>NPRL3</i> -R: GGTACCTGAACAGCAGC	N/A
<i>DEPDC5^{Flag}</i> knock-in cell line	sg <i>DEPDC5</i> - F:caccTGCAAGATGAGA ACAACAA sg <i>DEPDC5</i> -R: aaacTTGTGTCTCATCT TGCAc	N/A
<i>DEPDC5^{Flag}</i> knock-in cell line	SSODN: GGAGGCAAGATGACTTC TCTGCCCAAGCT TGGAACAGCTAAAGGG AAAAACAGTGCAA GATGGACTACAAAGACC ATGACGGTGATT ATAAAGATCATGACATT GATTACAAGGATG ACGATGACAAGGCGGCC GCAGGCCGTACG ACGAAAAGTCTACAACT CGTCATCCACAAG AAGGGCTTTGGGGCA GTGGTCA	N/A
<i>DEPDC5^{Flag}</i> knock-in cell line validation	<i>DEPDC5</i> -F: TTCCGAGAGTCACTTGG CAC <i>DEPDC5</i> -R: AGTCGCCTGTTTA GCCTCAAT	N/A
<i>WDR24^{Flag}</i> knock-in cell line	sg <i>WDR24</i> -F: caccgCACACGGGACATCT TCTCCA sg <i>WDR24</i> -R: aaacTGGAGAAGATGTCC CGTGTc	N/A
<i>WDR24^{Flag}</i> knock-in cell line	SSODN: CTGACCAGGCCAGCCCCA CCTCACTGACCTC CTGACCCCTGACCTCAT CACCTGTGCAGCC ATGGACTACAAAGACCA TGACGGTGATTAT AAAGATCATGACATTGA TTACAAGGATGAC GATGACAAGGCGGCCG CAGGCGAAAAAAT GAGCCGAGTACCACAG CCCTGGGTGGCA GCGTGCTGACAGG	N/A
<i>WDR24^{Flag}</i> knock-in cell line validation	<i>WDR24</i> -1F: AGGTCTGAACTGATGAC	N/A

REAGENT or RESOURCE	SOURCE	IDENTIFIER
	<i>WDR24</i> -1R: GGAGCATCCAAGGTGGC AG	
<i>WDR24^{C743A/C746A}</i> knock-in cell line	sg <i>WDR24</i> -F: caccgGTCTGCCACCACGT AGTCAA sg <i>WDR24</i> -R: aaacTTGACTACGTGGTG GCAGACc	N/A
<i>WDR24^{C743A/C746A}</i> knock-in cell line	SSODN: TCGGGAGGTGGGGCAG GGCCTGCAGGCA GCGCAGCAGCCCCGCT GAGGCACCCCTCCC TCCCGCCGCCCCAGG TGCCACCGCTGCG CCAGCATGGCCGCCGTC GCCACCATGTAG TCAAGGGTCTCTTCGTG TGGTGCCAGGGCT GCAGCCACGGCGCCA CCTGCAGCACATC ATGAAGTGGCTGGAAG GCAGCT	N/A
<i>WDR24^{C743A/C746A}</i> knock-in cell line validation	<i>WDR24^{CA}</i> -F: CTGCACGTCAACTGCAG C <i>WDR24^{CA}</i> -R: GGAGTACTCGCA GAGGTG	N/A
<i>WDR59^{C924A/C927A}</i> knock-in cell line	sg <i>WDR59</i> -F: caccgCCAGTGTGCCATCT GTCACG sg <i>WDR59</i> -R: aaacCGTGACAGATGGCA CACTGGc	N/A
<i>WDR59^{C924A/C927A}</i> knock-in cell line	SSODN: AGTTCGGCGTGTACTGC AGCCACTGCCGGA GTGAGGTCCGTGCCACG CAGTGTGCCATCT GCAAAGGCTTCACGTTT CAGGCCGCCATCG CCCACGTGGCTGTGCGG GGATCGTCCAATT TCTGCCTGACCTGTGGG CACGGTGGCCACA CCAGCCACATGATGGAG TGGTTTCGGACCC AGGAGGTGTGTCCCACC GGG	N/A
<i>WDR59^{C924A/C927A}</i> knock-in cell line validation	<i>WDR59^{CA}</i> -F: GAGTCTTGAGAGGAAG ACTTC <i>WDR59^{CA}</i> -R: GCT TGTACCCGGCACTTATG G	N/A
<i>WDR24^{-/-}</i> mice	gRNA1:- 5'- GTGCTTTGACCTCCGAA GGAAGG-3' gRNA2-5'- GACTCTGTACGACCTT CTCTGG-3'	N/A

REAGENT or RESOURCE	SOURCE	IDENTIFIER
<i>Wdr24</i> ^{C743A/C746A} knock-in mice	gRNA1:- 5'- ATGGCAGACAGCACACA TGCTGG-3' gRNA2-5'- GTGTGCTHTCTHCCAAT CATGTGG-3'	N/A
<i>Wdr24</i> ^{C743A/C746A} knock-in mice oligo	GCTCCCCAGCTGAACAG CCCTCCCATTTCCC AGGTGCCACCGCTGTGC CAGCATGGCCGCT GTCGCCATCATGTGGT TAAAGGCCTGTTC GTGTGGTGCAGGGTTG CAGTCATGGTGGC	N/A
PCR primers used for <i>Wdr24</i> ^{-/-} mice	F-5' AAGATTTATGCCATT GAGGA-3' R-5'- ACTCTTTCTGGGCTGTT CC-3'	N/A
PCR primers used for <i>Wdr24</i> ^{Ring/ Ring} mice	F-5'- CTTCTGCCTCTGGAATG TG-3' R-5'- TAAGGGGCTGTGAGCCT AG-3'	N/A
UBE2A-siRNA	siRNA1: ACCTCCCTACTCCTGTC ATTA siRNA2: GTCTATGCAGATGGTAG TATA	N/A
UBE2B-siRNA	siRNA1: GCAGTTATATTTGGACC AGAA siRNA2: CGGGATTCAAGCGGTT ACAA	N/A
UBE2C-siRNA	siRNA1: CCCTTACAATGCGCCCA CAGT siRNA2: GCCTGTCCTTGTGTCGT CTTT	N/A
UBE2D1-siRNA	siRNA1: CTTCTTTCTCACTGTACA TTT siRNA2: GCGATCCACCTGCTCAC TGTT	N/A
UBE2D2-siRNA	siRNA1: TGCCATCTGTTCTCTGT TGT siRNA2: GTTCTCTGTTGTGTGAT CCCA	N/A
UBE2D3-siRNA	siRNA1: CCAGAGATTGCACGGAT CTAT siRNA2: GCCTGCTTTAACAATTT CTAA	N/A
UBE2D4-siRNA	siRNA1: CTAGAGATTGGGTCAT GTTA siRNA2:	N/A

REAGENT or RESOURCE	SOURCE	IDENTIFIER
	CACCCTAATATCAACAG CAAT	
UBE2E1-siRNA	siRNA1: GCAAACCGAGAAAGAA ACAAA siRNA2: GTCCAGCACTAACCATT TCTA	N/A
UBE2E2-siRNA	siRNA1: CCGATGGAGATCAACGT GAAA siRNA2: CCGCTGCTAAATTGTCA ACTA	N/A
UBE2E3-siRNA	siRNA1: CGGACTTCTGTGTATATG TTA siRNA2: CCACTGCTAAGTTATCC ACTA	N/A
UBE2G1-siRNA	siRNA1: GCTAATGTTGATGCTGC GAAA siRNA2: CGATGGGAAGTCCTTAT TATT	N/A
UBE2G2-siRNA	siRNA1: GAGATTTACCTGTGAGA TGTT siRNA2: GATGAGATTTACCTGTG AGAT	N/A
UBE2H-siRNA	siRNA1: CTTCATGTTCTGGTTTG GTTT siRNA2: TACGATCCTGGGAGGAC TTAA	N/A
UBE2J1-siRNA	siRNA1: GATGATATACCTACAACA TTC siRNA2: ACATTCTGCATTGGGTAT AAT	N/A
UBE2J2-siRNA	siRNA1: GAAGTCGTGGAGGAGAT TAAA siRNA2: GTGTCTTTCTATCACGG ATTT	N/A
UBE2K-siRNA	siRNA1: TGACTCTCCGCACGGTA TTAT siRNA2: TACCAGAAACATACCCA TTTA	N/A
UBE2L3-siRNA	siRNA1: CCACCGAAGATCACATT TAAA siRNA2: CCAGCAGAGTACCCATT CAAA	N/A
UBE2N-siRNA	siRNA1: AGACAAGTTGGGAAGA	N/A

REAGENT or RESOURCE	SOURCE	IDENTIFIER
	ATATG siRNA2: CCATAGAAACAGCTAGA GCAT	
UBE2O-siRNA	siRNA1: TCGTCATCCGCATCGGC AATA siRNA2: ATGTGAGTGTTCACGAC ATTG	N/A
UBE2Q1-siRNA	siRNA1: CACTATGAAATGAAAGA GGAA siRNA2: GCCAACAAATCTCAATA CAGT	N/A
UBE2Q2-siRNA	siRNA1: CCATTTGTTTCGAGTGGT GTTA siRNA2: GAGCCCAACAATCCTAT AATT	N/A
UBE2QL1-siRNA	siRNA1: GTTTGGTGAAGACGCAT GAAA siRNA2: CCTGTTCCGACTGGAACG TGAA	N/A
UBE2R1-siRNA	siRNA1: GAGTGTGATCTCCCTCC TGAA siRNA2: GGTGGACGAGGGCGAT CTATA	N/A
UBE2R2-siRNA	siRNA1: CCAAATGTCGATGCTTCA GTTA siRNA2: GCCGACTGTTATGATGA TGAT	N/A
UBE2S-siRNA	siRNA1: GGGCTCTCTCCTCCTT CCAC siRNA2: TGGGCTCTCTCCTCCT TCCA	N/A
UBE2T-siRNA	siRNA1: TGAGGAAGAGATGCTTG ATAA siRNA2: TTGTCTGGATGTCTC AAAT	N/A
UBE2U-siRNA	siRNA1: CCTCCAGTTGTGAAATT TATA siRNA2: GCATCAGAAAGAATGGA ATTT	N/A
UBE2V1-siRNA	siRNA1: CCAAGAGCCATATCAGT GCTA siRNA2: AGGACAGTGTACAGCA ATTA	N/A

REAGENT or RESOURCE	SOURCE	IDENTIFIER
UBE2V2-siRNA	siRNA1: GTCTTAAATCAACAACC TTCT siRNA2: CAAGGTGGACAGGCATG ATTA	N/A
UBE2W-siRNA	siRNA1: CGCTCTCAGTCCAATCA GTTT siRNA2: GCATGAATTAACATGCG TCTT	N/A
UBE2L6-siRNA	siRNA1: GCTGGTGAATAGACCGA ATAT siRNA2: GATCAAATTCACAACCA AGAT	N/A
UBE2Z-siRNA	siRNA1: GCGGGATATCATGTCCA TTTA siRNA2: GTTTCTCCTGTTCTGTT TTTC	N/A
NEDD4-shRNA-1	CCGGAAGAATTATGGGTG TCAA	N/A
NEDD4-shRNA-2	CCGTCAAGTAAGTTGGA TGTT	N/A